ANALYSIS OF BLOOD PRESSURE WAVEFORM FOR DETECTION AND DIAGNOSIS OF CARDIOVASCULAR ANOMALIES

by

ATUL SHROTRIYA

Presented to the Faculty of the Graduate School of
The University of Texas at Arlington in Partial Fulfillment
of the Requirements for the Degree of

MASTER OF SCIENCE
in
MECHANICAL ENGINEERING

THE UNIVERSITY OF TEXAS AT ARLINGTON
December 2021

To my mother Sunita and my father Anil K. Shrotriya for their unwavering support.

To my professors at the University of Texas at Arlington (UTA) who molded me into a reliable engineer and researcher.

To my colleagues, peers, mentors and friends; especially at the Engineering Student Council UTA (ESC) through whom I was able to effectuate multitudes of opportunities to gain academic, leadership and other character development skills.

And to UTA, for this brilliant experience.

ACKNOWLEDGEMENTS

I would like to thank my supervising professor Dr. David A. Hullender for constantly motivating and encouraging me throughout the research. I am also grateful for his invaluable advice during the course of my graduate studies. His directions were crucial for me to gain the necessary skills and background knowledge to complete this research.

I wish to thank my academic advisor Dr. Seiichi Nomura for his constant guidance and for his interest in my research and for taking time to serve in my thesis defense committee. Dr. Nomura and Dr. Hullender have also been a great help throughout my academic journey at the University of Texas at Arlington and his encouragement has allowed me to receive multiple scholarships, present at conferences and obtain graduate teaching assistant and internship opportunities among other benefits.

I am grateful to Dr. Robert Woods taking the time to discuss my research on multiple instances, for serving on my thesis defense committee and for the invaluable knowledge regarding practical applications of control systems through his course Control System Components.

I would also like to extend my appreciation towards all of my professors at the University of Texas at Arlington, especially Dr. Frank L. Lewis and Dr. Michael Niestroy who taught me advanced techniques in control systems. Dr. Lewis and

Dr. Niestroy are from the Department of Electrical Engineering and their courses along with keen attention were pivotal for me to connect the mechanical systems and knowledge of control systems to real-world modern applications. They also motivated me to pursue independent research projects under their supervision which allowed me to have multiple perspectives of control system implementations.

I would also like to thank the faculty and staff at the University of Texas at Arlington and the Department of Mechanical Engineering. While I cannot possibly name all the people who have helped me throughout my journey at UTA, some of these people are Dr. Carter Tiernan, Tracey Faulkinbury, Dr. Teik C. Lim, Dr. Sunand Santhanagopalan, Dr. Hyejin Moon, Dr. Stephen Evans, Delania Gordon and Wendy Ryan.

Finally, I would like to express my deep gratitude to my parents who permitted me to pursue my graduate studies in the United States and empowered me to perform at an exceptional level. I am extremely fortunate to have brilliant mentors and friends at the Engineering Student Council (ESC) at the University of Texas at Arlington. They honed my skills and enabled me to become a better person. I also thank several of my colleagues, peers, friends and mentors who have helped me throughout my career.

December 1, 2021

ABSTRACT

ANALYSIS OF BLOOD PRESSURE WAVEFORM FOR DETECTION AND DIAGNOSIS OF CARDIOVASCULAR ANOMALIES

Atul Shrotriya, M.S.

The University of Texas at Arlington, 2021

Supervising Professor: Dr. David A. Hullender

Cardiovascular diseases are the leading cause of mortalities worldwide as well as in the United States. Early diagnosis and prediction of these diseases is critical to mitigate the risks to the patient. A common method to assess a person's heart health is through the use of cuff type oscillometric devices placed on the arm of the patient. As the mean pressure in the cuff is increased the blood flow in the brachial artery becomes blocked. When the cuff pressure is reduced the blood starts flowing again; during this cycle, pressure fluctuations in the cuff are measured using a pressure transducer. Modern devices use proprietary algorithms on these pressure fluctuations to estimate a patient's systolic and diastolic pressure levels. Hullender and Brown developed a model and an extended Kalman filter algorithm which is able to estimate the total blood pressure waveform along with arterial stiffness component using the same cuff pressure fluctuations. This research pertains to an evaluation of the algorithm for different levels of measurement uncertainty and different mean pressure cuff levels and cycle rates.

This work also develops and evaluates an extension of the algorithm to assess the cardiovascular health of a patient. The extended algorithm uses standardized values for a blood pressure waveform to diagnose cardiovascular anomalies such as high blood pressure, hypertension severity, arrhythmia, atrial fibrillation, tachycardia and bradycardia. It also extracts important blood pressure waveform characteristics such as time periods and their ratios associated with different peaks in each cycle, dicrotic notch depth, systolic pressure increment and detriment slopes along with ventricular and total cardiac output factors. Furthermore, these characteristics are measured continuously and their average and variations are provided in the final diagnostic report. While the measured characteristics are not as obvious as the diagnosed anomalies, they can be viewed by a medical professional for quick diagnosis instead of having to analyze each parameter by studying the waveform. The significance of these preliminary results to assess the cardiovascular health of a patient appears to be most promising and justification for future research considering complexities associated with patient-to-patient differences, levels of patient activity, effects of other medical issues, etc.

TABLE OF CONTENTS

LIST OF ILLUSTRATIONS

LIST OF TABLES

CHAPTER 1

INTRODUCTION

Cardiovascular diseases are the leading cause of death worldwide and in the United States as per the data published by the World Health Organization and National Center for Health Statistics (US) in 2019 [1, 2]. As per these reports, over 17.9 million people died due to heart diseases worldwide which accounted for 32 percent of all deaths globally. More than 75 percent of these deaths occur in countries which have low or middle-income.

Heart diseases are also a major concern in the United States where they are the leading cause of death as per a 2019 report published by the National Center for Health Statistics. 1 out of every 4 deaths in the United States occurred due to heart disease in 2019. According to the NCHS report, heart diseases caused 659,041 and another 150,005 people died due to stroke in the US [2]. Over $363 billion were lost in 2019 due to heart diseases, these costs not only include the hospital bills but also the work lost when the patients weren't able to contribute to the US economy. In the latest estimates published by National Vital Statistics System, heart disease had caused twice the number of deaths as compared to the COVID-19 pandemic during the year 2020 [3]. This data proves that cardiovascular diseases are the most significant challenge for the healthcare industry as of present.

1.1 Major Cardiovascular Diseases

Worldwide, more than 85 percent of the deaths associated with heart diseases occur due to heart attacks and strokes [4]. Ischaemic (or ischemic) heart disease which

is also known as coronary artery disease or coronary heart disease is the leading cause of mortality across the world as per the latest data published in 2019 by the World Health Organization. This is followed by stroke which makes the top two causes of mortality related to cardiovascular ailments. Ischaemic heart disease caused 8.9 million deaths and 6.1 million people died due to strokes in 2019 [1].

In the United States as well, coronary artery disease accounts for more than 50 percent of all deaths associated with heart diseases [5]. Nearly 6.7 percent of all adults over the age of 20 years have this disease in the US. Heart attacks are another major concern relating to heart diseases, in the US around 805,000 people have a heart attack each year and every 40 seconds someone has a heart attack. One out of every five heart attacks is silent and the patient has no idea of its occurrence or the damage caused to their heart [5, 2].

1.1.1 Ischaemic Heart Disease

As defined by the American Heart Association, all parts of our body need oxygen to function properly which is supplied through blood. When the blood flow is reduced or restricted within a part of the body, it is termed as ischemia. When the blood flow to heart is reduced, the condition is termed as cardiac ischemia.

Heart problems arising from the narrowing of heart arteries is termed as ischaemic heart disease which can cause heart attacks ultimately. Commonly, ischaemia causes pain or discomfort in the chest region which is medically referred to as angina pectoris. However, in many cases ischemia can also occur without pain which is termed as silent ischaemia and can cause silent heart attacks [6].

1.1.2 Contributing Factors to Cardiovascular Diseases

The effects of cardiovascular diseases or risk of developing a heart disease can be compounded by age, family history, lifestyle and presence of other diseases. The key risk factors for cardiovascular diseases include smoking, diabetes and cholesterol. Around 47 percent of all Americans have one of these three key risk factors [5]. According to the Center for Disease Control in the United States, 10.5 percent of total population and 13 percent of adults over the age of 18 years suffer from diabetes [7].

Patients with other health conditions like diabetes, obesity and chronic kidney disease (CKD) are at a higher risk of getting cardiovascular diseases and they also have higher chances of cardiovascular incidents along with mortality rates [7, 8]. Similarly, heart disease can also lead to other health conditions which makes it important to diagnose cardiovascular diseases as early as possible for risk mitigation and early action to stop or slow additional damage.

1.2 Common Cardiovascular Assessment Techniques

Growing pace of technology is becoming more focused on healthcare and diagnostics technology. Further advancement of manufacturing techniques and computational resources improved diagnostic processes through wearable devices which allow for continuous health monitoring of patients [9, 10]. However, measuring blood pressure is a basic check performed by medicine professionals.

This check is essential and supplementary to a wide array of diagnostic procedures. In many cases requiring blood pressure tracking, patients often use remote kits for doing the test themselves. These readings are then reported to the consulting doctor. Modern devices including but not limited to smartwatches and fitness bands

provide a convenient means to measure blood pressure [11, 12, 13]. They can also be used for monitoring the blood pressure of a patient while they are sleeping or access it continuously to diagnose any irregularities such as arrhythmias. Further research is being done to develop wearable devices and algorithms which can provide better readings remotely [14, 15, 16, 17]

Among the most common procedures for measuring the blood pressure, a cuff type device is placed on the upper portion of the arm where the brachial artery is present. Then the pressure in the cuff is increased till it completely blocks off the flow in the artery. After this, the pressure is reduced which allows the blood to flow again. This causes pressure fluctuations in the cuff which are measured using pressure transducers. Commercially available devices use proprietary algorithms to estimate the blood pressure using these cuff pressure fluctuation measurements. The cycle of increasing and decreasing the blood pressure can be repeated more than once. However as per a 2014 study, even advanced blood pressure measurement systems only provide the systolic and diastolic pressures in most cases and are unable to take advantage of the entire blood pressure waveform [18].

1.2.1 Hullender and Brown's Waveform Estimation Algorithm

In a 2020 paper, Hullender showed that an extended Kalman filter yielded promising results to estimate the blood pressure waveform [19]. Furthermore, it is reported that arterial stiffness and hypertension can also be calculated using the blood pressure waveform. This research first evaluates the algorithm developed by Hullender and Brown. This is followed by developing an extension to the algorithm that just uses the estimated blood pressure waveform to extract the important blood pressure waveform characteristics and then compares some characteristics to standardized values for diagnosing high blood pressure, hypertension severity, arrhythmia, atrial

fibrillation, tachycardia and bradycardia while reporting others. It should be noted that the extension to the algorithm can work independently by just assessing the blood pressure waveform. In case a different algorithm is developed which can provide the blood pressure waveform using other means such as pulse wave velocity or optical sensors then the same extension developed in this research can be applied to those algorithms too. The algorithm developed by Hullender and Brown along with the techniques used such as Fourier transformation and extended Kalman Filter functioning are explained in detail in Appendix C.

1.2.2 Possible Enhancements for the Current Extended Kalman Filter Algorithm

Various studies have found that most of oscillometric devices fail to extract full information available in the blood pressure waveform [20, 21, 22]. However, Hullender and Brown's algorithm is reliably able to provide accurate estimates for the entire blood pressure waveform.

Blacher surmised that pulse wave velocity measurements can be used to detect hypertension in patients [23]. Similarly, the presence of measurement from other sensors can be used to verify the estimates especially in cases where the cuff type transducers seem inadequate due to physical limitations. Kalman algorithms can effectively utilize simultaneous signals from multiple sources such as pulse wave velocity (PWV) sensors or optical sensors found in most smartphone cameras [24]. Furthermore, the readings from different sensors can be combined to make better diagnoses as there will be more than one factors to indicate an anomaly.

1.3 Characteristics of Blood Pressure Waveform for Diagnosis

The blood pressure waveform is an ideal indicator for getting vital body signals especially during competitive events, diagnosing conditions linked to heart rate

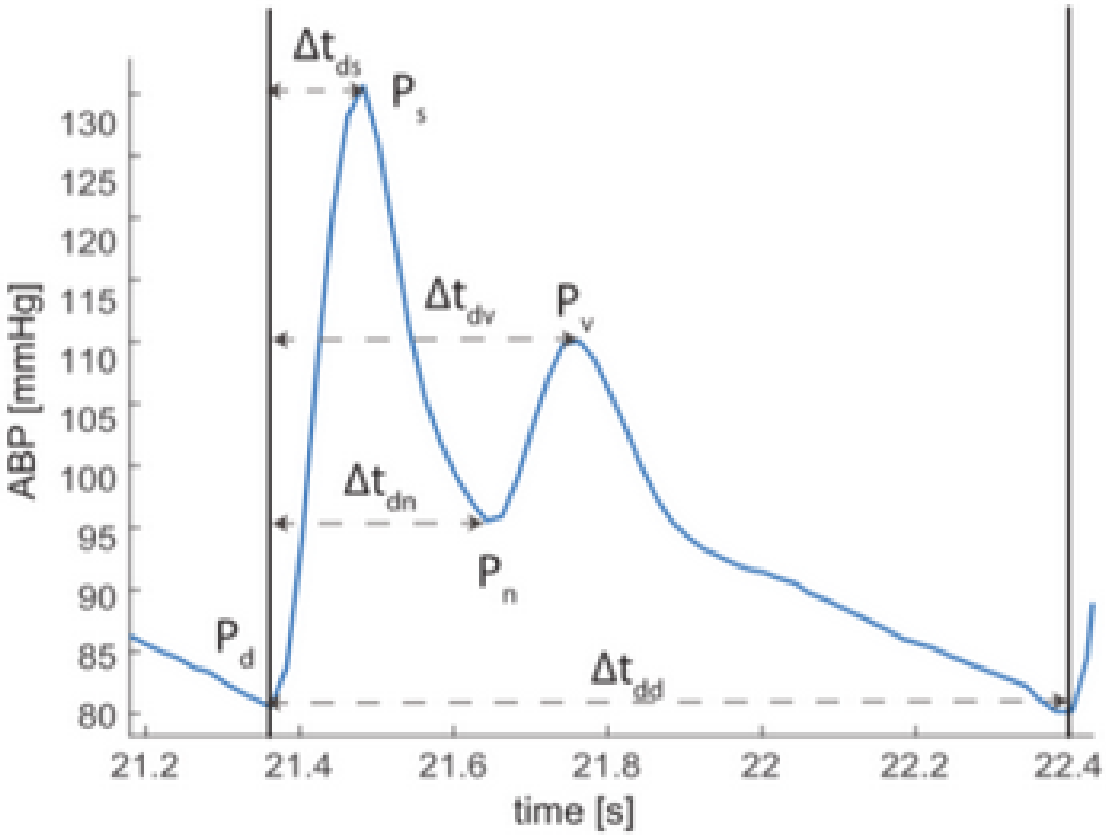

Figure 1.1. Normal Blood Pressure Waveform Cycle.

such as hypertension and even for non-medical applications such as overcoming public speaking anxiety or stuttering [25], improving sport performance etc. Various studies have been conducted to develop models for obtaining the blood pressure waveform [26, 19] or to analyze it for diagnosis of heart diseases [27, 28, 29, 30] Some important characteristics that can be utilized to predict heart conditions and diagnose cardiovascular diseases [31, 30] are explained using the figures [32] below.

The above figure depicts one cardiovascular cycle with normal characteristics [33]. Here, systolic pressure (P_s) is the pressure at the highest peak of the curve whereas the diastolic pressure (P_d) is the lowest pressure on the curve. These pressures are measured by most common devices and are useful for diagnosing hypertension and

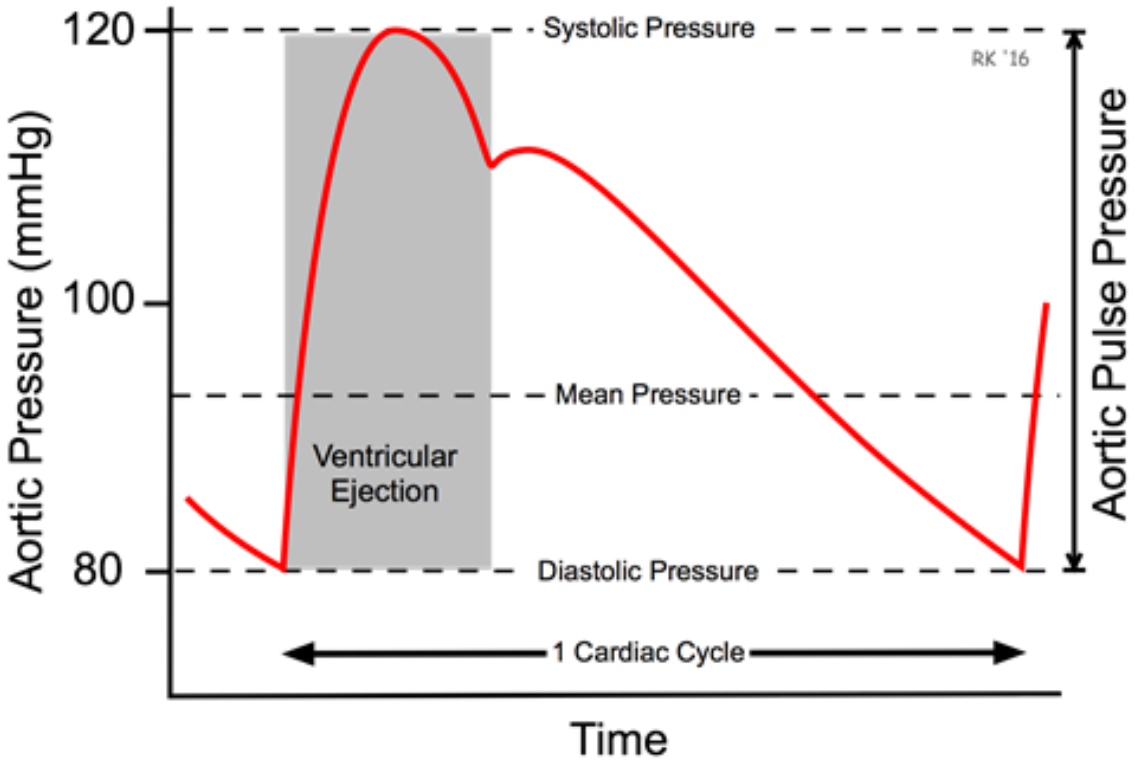

Figure 1.2. Ventricular Ejection Region on Blood Pressure Waveform.

assessing the risk for heart attack and stroke. The dicrotic notch (P_n) is the minimum pressure in the valley after systolic pressure and marks the end of ventricular ejection. The dicrotic peak (P_d) occurs right after the dicrotic notch. Combined, these two are important factors in predicting the cardiovascular output, aortic valve functioning, systole to diastole ratios and pressure reflections.

Other than these pressures, the time periods to reach these pressures along with the entire cycle time are important factors in detecting elevated heart rate and anomalies in cardiac output which can be used to predict or diagnose ischaemic heart disease [34]. Furthermore, the waveform can be used to calculate the slope of the systolic peak which is a good indicator of the arterial thickness and flexibility. A higher slope of the blood pressure waveform indicates thin-walled arteries requiring

minimal oscillations to change the pressure. Comparing all these characteristics over time can allow medical professionals to diagnose any sudden changes or look into any abnormalities [35, 36].

1.3.1 Parameters to consider while diagnosing

Cardiovascular diseases cost over 218 billion dollars and 138 billion dollars due to lost productivity every year [37]. It is difficult to quantify the exact number of incorrect diagnoses due to the variety of factors involved. However, various studies conclude that cardiovascular diseases are more prone to misdiagnoses [38, 39]. For cardiovascular malpractice cases with incorrect diagnoses, the chances of death are 75 percent as compared to 27 percent for non-cardiovascular diseases.

Diagnosing cardiovascular diseases can also have significant impacts on the lifestyle and overall mental state of the patients. In some cases, the blood pressure waveform might have slight fluctuations due to measurement errors or due to the functioning of the pressure transducers in the cuff type oscillometric device. Furthermore, the presence of other diseases or factors such as age, gender or body physique [40] may lead to changes in the blood pressure waveform. Therefore, it is important to consider such parameters while diagnosing and verify the data before any predictions are made.

To do this, the second chapter evaluates the performance of the algorithm developed by Hullender and Brown within different conditions before focusing on its implementations.

1.3.2 Impacts of better diagnosis of cardiovascular diseases

As per the American Heart Association and the World Health Organization, early diagnosis of cardiovascular diseases is crucial for timely action [37, 1]. This

can help to prevent the onset of certain heart diseases and significantly reduce the complications associated with long term cardiovascular damage [41].

According to a 2012 study, United States had the highest rates of unplanned re-hospitalizations following a myocardial infraction event [42]. Due to a high mortality risk, the United States government launched a program to penalize hospitals which had significantly higher unplanned readmission rates within 30 days as compared to the national average [43, 44].

Remote monitoring of patients is another challenge for medical professionals. Advanced methods such as the electrocardiograph or CT scan to accurately gain data about the patient's blood pressure require expert knowledge regarding the implementation and operation of such systems. Therefore, being able to assess the entire blood pressure waveform through simple cuff type oscillometric devices will greatly increase the capabilities for remote monitoring and diagnosis. Additionally, algorithms for extracting important characteristics from the waveform will further ease the work of medical professionals and save significant amount of time spent studying the readings from other instruments. The third chapter delves into developing algorithms that can be reliably used to extract important characteristics from the blood pressure waveform while diagnosing conditions which are based on standardized values unaffected by factors such as age, gender or body type under usual circumstances.

CHAPTER 2

SYSTEM TESTING

An erroneous estimation of the blood pressure waveform can lead to incorrect diagnoses of patients. As explained in the previous sections, faulty diagnoses pose a huge risk to the patients especially in the case of cardiovascular diseases. While the equations for modeling the system have been verified to be accurate, this section deals with assessment of algorithm's performance, limits and control methods. This is done to check the convergence rate and computational resources used by the algorithm under different conditions followed by an assessment of errors at extreme limits.

2.1 Optimal Control of Estimation System

The blood pressure waveform is estimated using the algorithm developed by Hullender and Brown as explained in previous sections. The algorithm uses an extended Kalman filter and it only uses one input which is the change in mean cuff pressure as it is inflated and deflated in cycles. The limits of the cuff pressure level are accurate as they represent the maximum pressure necessary to cut off the blood flow in the brachial artery and the minimum pressure is zero. Henceforth, various methods are evaluated for controlling the rate of pressure change (r) within the cuff pressure excluding the pressure fluctuations.

The main aim of optimally controlling the rate of pressure change in the cuff is to reduce computation requirements and to achieve convergence between the real and estimated values quickly. Furthermore, the extended Kalman filter estimation algorithm is tested for error, covariance and noise limits at different rates of cuff

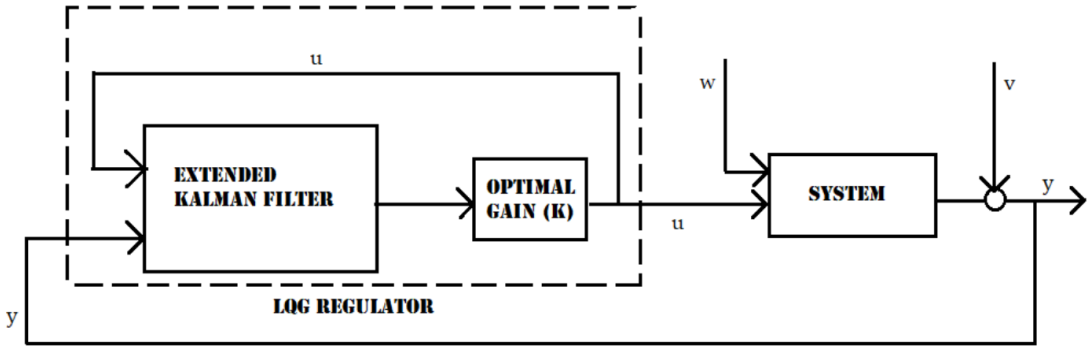

Figure 2.1. Diagram for an LQG regulator.

pressure change (r) and with different measurement noise covariance values which are specified using the R matrix in most Kalman filters.

2.2 Optimal control of cuff pressure fluctuations

The cuff pressure variation was analyzed to assess its impact on the convergence of the extended Kalman Filter algorithm. The Kalman Filter to estimate the 16 parameters is an extended Kalman filter. The parameters to be estimated are the 11 Fourier series coefficients, frequency ω, cuff pressure fluctuations along with artery volume and its parameters i.e., V_{ao}, a and b. The system locally linearizes the non-linear equations and computes estimates and is not applicable for severely non-linear systems. To optimize this, a linear quadratic regulator (LQR) approach is attempted with constrained control as the cuff pressure input is limited by maximum pressure and pressure change rate. This system can be generally described by the LQG regulator diagram in Figure 2.1.

In Figure 2.1, v is the measurement noise and w is the process noise. The input to the system is u and the output is y. To formulate the optimal gain through LQR, the first step is to define a cost function which needs to be extremized. On evaluating the above equations, it is anticipated that optimally varying the low frequency portion

of pressure inflating and deflating the cuff would lead to more accurate estimates from the Kalman algorithm. Simulations of the combined optimally controlled low frequency portion of the cuff pressure in conjunction with the Kalman filter algorithm are used to assess the potential improvements in robustness and accuracy of the concept.

The maximum volume of cuff is 100 cm^3 whereas the initial volume is 20 cm^3. The constants 'a' and 'b' may vary from equipment to equipment and are kept as 0.075 and 0.02 respectively in mmHg units. For comparison, the normal artery has the same parameters as 0.11 and 0.03. The actual artery volume at 0 transmural pressure is 0.25 cm^3 and initial estimate is 0.3 cm^3.

2.2.1 Controller Design

Since the measured output is cuff pressure variations, it seems likely that a higher magnitude of these variations would result in more information for the Kalman filter leading to better estimates. Therefore, a graph is plotted (shown in figure 2.2) between estimated cuff pressure ($P_c(t)$) which is the input and the estimated cuff pressure variations(y(t)).

From the graph in figure 2.2, it appears that there are three options for optimization:

1. The maximum amplitude of $\dot{y}\ (t)$ which is around 160 mmHg i.e., maximum cuff pressure (P_{cm})
2. The maximum variation in amplitude of y(t) which is around 80mmHg
3. On closer inspection of the graph and comparing it to the blood pressure waveform, it is observed that the maximum amplitude difference around 80 mmHg is achieved as it corresponds to the diastolic blood pressure. This is readily observable from the $\dot{y}\ (t)$ equation. Here, the compliance function ($f(P_t)$) decreases

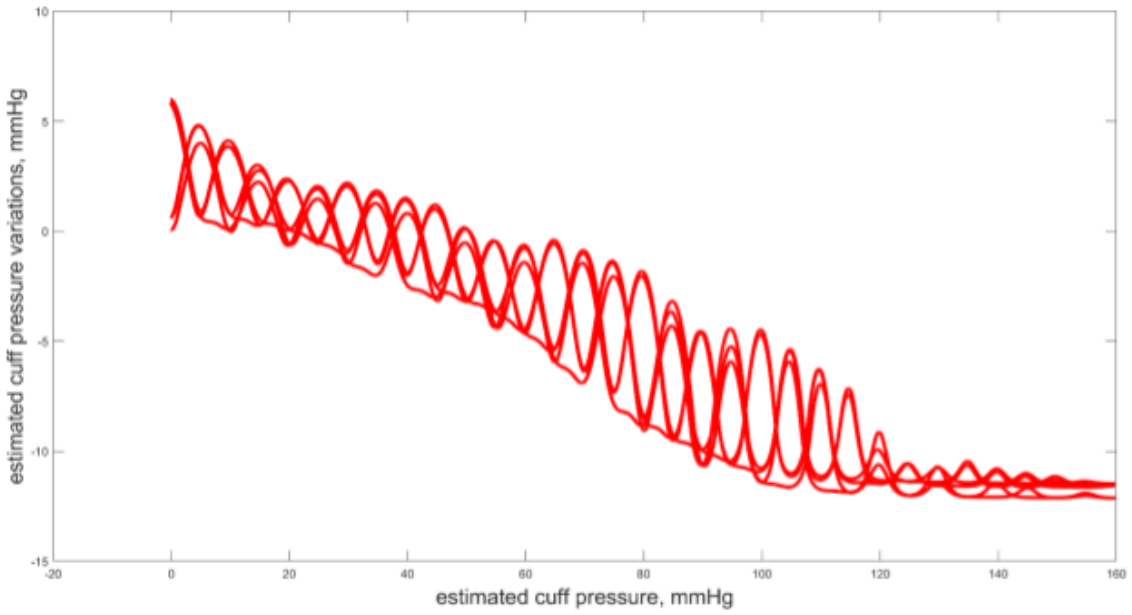

Figure 2.2. Relation of variations in cuff pressure to the cuff pressure.

for any value of transmural pressure above 0. Similarly, if the cuff pressure (P_c) is stabilized then the only contribution to $\dot{y}\ (t)$ would be through the change in blood pressure. This will reduce the bias due to input. Therefore, a controller can be designed to maintain the cuff pressure near to the diastolic pressure based on the average diastolic pressure obtained from previous Kalman filter estimates. As the readings proceed, the average will stabilize which will lead to better control and estimation.

Research studies show that human body can withstand sudden external pressures of nearly 40 psi or more than 2000 mmHg without damage. Air pressures of 5 psi or nearly 260 mmHg directly to the eardrum can cause damage in 1 percent of cases [45, 46, 47, 48, 49]. From the above graph, it is apparent that increasing the cuff pressure to nearly 160 mmHg results in the maximum magnitude of cuff pressure variations which are then used by the extended Kalman filter to generate estimates.

Cost functions to be maximized are:

$$J1 = \int_{t0}^{tf} y(t)\,dt \qquad \text{for the first optimization option,}$$

$$P_c(tf) = 160mmHg; \qquad \text{terminal constraint for } J1 \text{(hard constraint)}$$

$$J2 = \int_{t0}^{tf} \frac{dy(t)}{dt}dt = \int_{t0}^{tf} dy(t) \qquad \text{for the second optimization option,}$$

$$P_c(tf) = 80mmHg; \qquad \text{terminal constraint for } J2$$

$$P_c(t) \leq |Pqm|; \qquad \text{input constraint}$$

Pqm is determined by Qmax or maximum airflow rate into the cuff.

Cost function to be minimized is:

$$J3 = \psi\big(P_c(tf)\big) + \int_{t0}^{tf} (P_c - P_d(t))^2 dt \qquad \text{for the third optimization option}$$

$$P_c(t) \leq |Pqm|; \qquad \text{input constraint}$$

$$\text{for } i = 1 \text{ to } n, \text{if } \dot{P}(t) = 0 \text{ and } \ddot{P}(t) > 0 \text{ then,}$$

$$P(t) = P_{di}(t)$$

$$P_d(t) = \frac{1}{n}\sum_{i=1}^{n} P_{di}(t)$$

Figure 2.3. Initial Algorithm for Optimal Control of Cuff Pressure Variation.

However, a cuff pressure of 160 mmHg which is around 3psi doesn't cause any harm to humans even if it's applied suddenly. It must be noted that sudden increase doesn't correspond to an impulse as it would generate a pressure increment in the form of blast overpressure which can cause injuries at values of 3psi. Since this is not applicable practically, the only limitation to reach a pressure of 160mmHg is the maximum air input to the cuff.

The quick pressure increment may not be suitable for a few extremely fragile patients but in that case even the conventional oscillometric devices may not be a good choice. Hence, a cost function with input constraint based on maximum air input to cuff can be defined to bring the cuff pressure to 160mmHg within a finite duration. This duration would be the time step used by the Kalman filter so that the next incoming value doesn't interfere with the current optimal input.

Here, Pd(t) is the average diastolic pressure based on previous values and n is defined by the number of estimations available. The input constraint remains the same as it is only dependent on maximum air input. Square values are taken so that the magnitude is minimized instead of the system trying to make the cuff pressure zero. Also, a soft constraint is specified to ensure that the system moves in the correct direction this may not be necessary as the diastolic pressure will dictate the direction adequately.

2.2.1.1 Noise cancellation approach

After discussion with Dr. Robert L. Woods, it was concluded that the cuff system cannot be modeled as an isolated lumped parameter system containing gases with variations caused due to blood pressure oscillations as noise. Thus, the system may not be adequately controllable using the Linear Quadratic Tracker approach.

A better approach would be the use of Model Predictive Control (MPC) techniques as they can handle interaction between input and outputs. However, they have limitations for long calculations as explained by Dr. Kamesh Subbarao in the Optimal Controls lectures at the University of Texas at Arlington. MPC can be integrated into the Kalman filter over a few steps to provide feasible solution. This would require extensive modification of MPC and local linearization of function.

The system is remodeled to exclude the variations considering them to be small and non-detrimental to the average pressure within the cuff.

2.2.1.2 System remodeling

The system is remodeled using the lumped parameter modeling approach [50]. The equations for temperature and density variation are neglected considering that

they don't have much impact. Implementing the capacitance equation for cuff pressure gives equation 2.1.

$$\dot{P}_c = 1.2 * \frac{P_c}{V_0 + ut}(-0.18u), \tag{2.1}$$

Here, P_c is the cuff pressure and u is the input provided to optimize it. Note, the heat transfer coefficient is kept 1.2 to give mid-range values. The above equation is not linear or an ordinary differential equation as there are two unknowns being multiplied. Therefore, the traditional methods are not applicable in this case. Combining different approaches taught by Dr. Subbarao, equations 2.2 to 2.6 can be derived.

$$P_c = c1 * (V_0 + ut)^{\frac{-0.22}{u}}, \tag{2.2}$$

Assuming the system takes 4 seconds to reach the pressure of 80mmHg, calculating and substituting the initial and final conditions,

$$1.609 = -0.22(ln(4 * u + V_0) - ln(V_0)), \tag{2.3}$$

This gives u 0 which cannot take the system anywhere in the desired time. Therefore, the usual methods are not applicable in this case. On trying the conventional two-point boundary value approach,

$$Hessian(H) = (P_c - 80)^2 + \lambda \frac{-0.22 P_c u}{V_0 + ut}, \tag{2.4}$$

$$\frac{\partial H}{\partial x} = -\dot{\lambda} = 2(x - 80) - \frac{0.22\lambda u}{V_0 + ut}, \tag{2.5}$$

$$\frac{\partial H}{\partial u} = -\frac{0.22\lambda V_0 P_c}{V_0 + ut} = 0, \tag{2.6}$$

This implies that $\lambda = 0$ and doesn't provide a reliable solution.

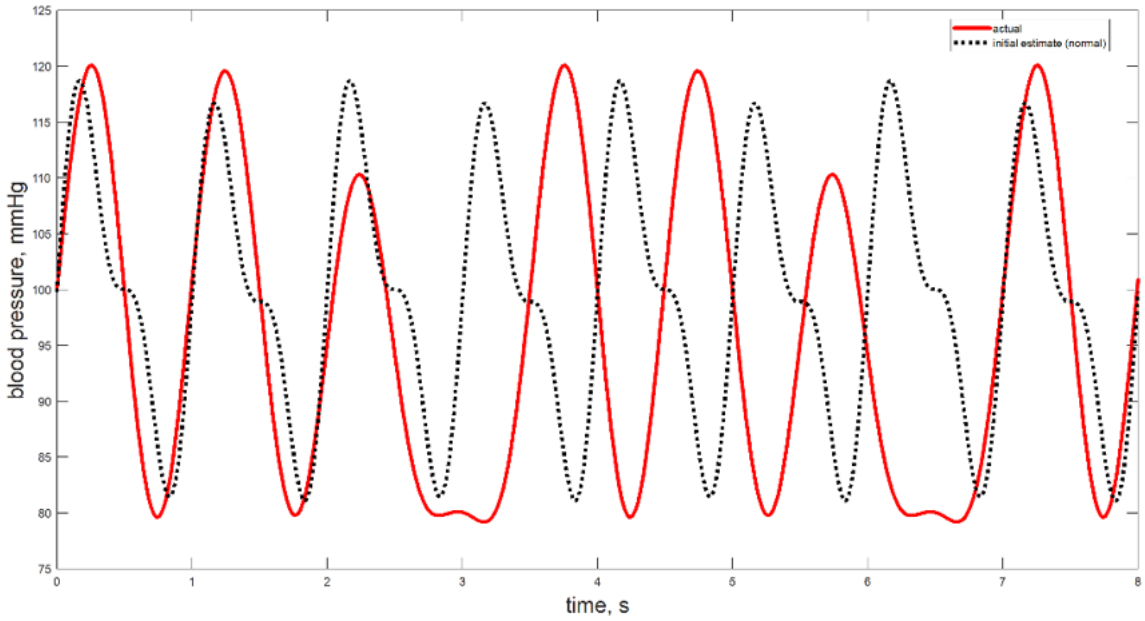

Figure 2.4. Real and estimated blood pressure values after using MATLAB Loop.

2.2.1.3 MATLAB loop

Another approach is attempted by simply choosing control effort (u) as the difference between current and target value (80mmHg) of cuff pressure. This is implemented using a for loop as follows:

```
for Pc>80
    u=-|Pc-80|;
for Pc<80
    u=|Pc-80|;
else u=0;
```

The above loop was added to the extended Kalman filter at the position where it stores values for P_c and the plot in Figure 2.4 was obtained.

From the above plot, it appears that there is a slight improvement in the rate of convergence. On the other hand, the estimate waveform is very different. Therefore, another similar approach was attempted using the following algorithm:

```
%The variable Pc is now independent of time and switches to
%either of the two thresholds which makes the rate of
%change of cuff pressure i.e., r=0

Pc=160*cf;
if t>Tf/nt && t<=2*Tf/nt
    Pc=0*cf;
elseif t>2*Tf/nt && t<=3*Tf/nt
    Pc=160*cf;
elseif t>3*Tf/nt && t<=4*Tf/nt
    Pc=0*cf;
elseif t>4*Tf/nt && t<=5*Tf/nt
    Pc=160*cf;
elseif t>5*Tf/nt
    Pc=0*cf;
end
```

As observed in Figure 2.5, the blood pressure waveform estimate is much better now. However, the peak values have a divergence of nearly 5mmHg which is not acceptable in most cases. It can be surmised that implementing bang-bang type control is making the system unstable due to sudden impulses in the input.

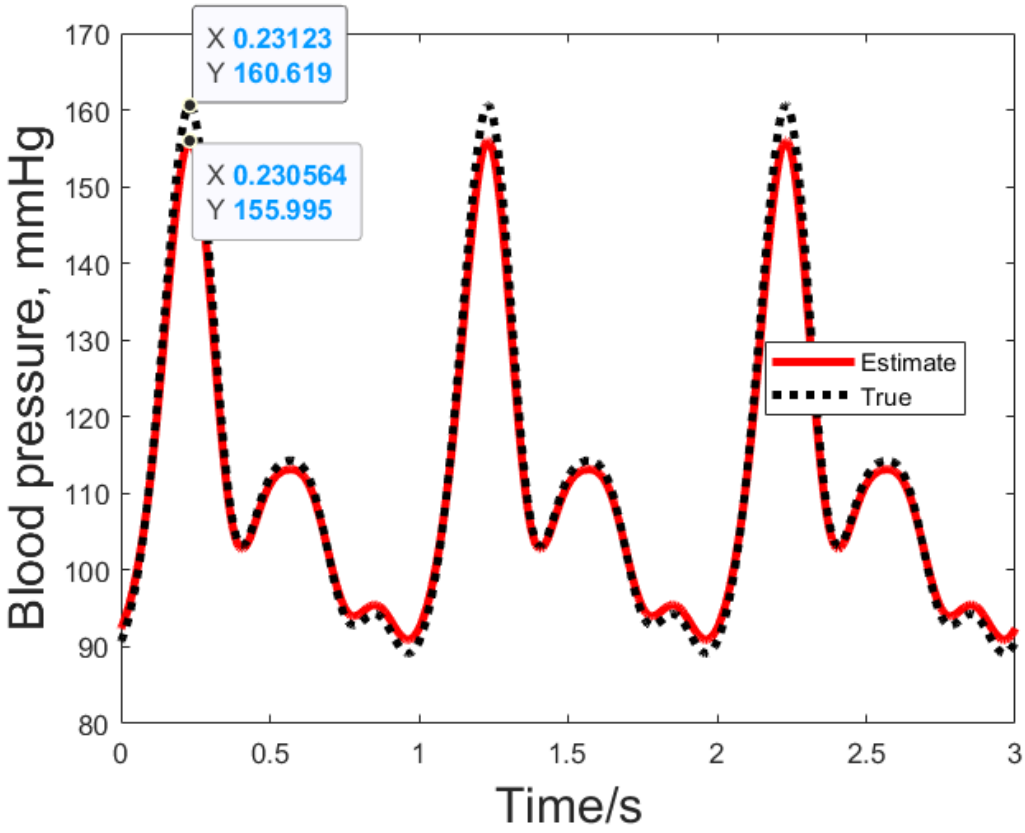

Figure 2.5. Estimated and True Blood Pressure Waveform with Bang-Bang Control.

2.2.2 Changing the r and cf values

As seen in the previous section, sudden impulses as input make the system unstable. So, the r and cf values are changed in an iterative manner to find the best value of cuff pressure variation which results in a low computation time while providing acceptable estimates for the blood pressure waveform.

2.2.2.1 Effect of number of cycles and cuff pressure rate on blood pressure waveform estimate

To check the impact of cuff pressure and cycles on the estimated blood pressure waveform, 8 different sets of values were tried using the design of experiment

methodology explained in Juran's Quality Handbook [51]. These included the values for r/cf and nt provided in Table 2.1

Table 2.1. Tests to assess impact of cuff pressure rate change and number of cycles on estimated blood pressure waveform

Trial Number	Cuff pressure variation factor (r/cf)	Number of cycles(nt)
1	15	4
2	10	6
3	15	6
4	7.5	8
5	10	8
6	6	10
7	8	10
8	10	12

The results showed that for above stated values there was no noticeable difference between the estimated and actual value once the extended Kalman filter system had converged for different values of cuff pressure fluctuations and number of cycles. Therefore, changing the rate of cuff pressure fluctuations slightly will not affect the quality of estimated blood pressure waveform. Thus, the next section focuses on the rate of convergence of the system along with the computational resources required for major estimated parameters to reach within 97.5 percent of actual value with the above shown trial values for number of cycles and larger values of cuff pressure change.

2.2.2.2 Effect of number of cycles and cuff pressure rate on convergence duration and computational requirements

From table 2.2 it is observed:

Table 2.2. Tests to assess impact of cuff pressure rate change and number of cycles on estimated blood pressure waveform

Cuff pressure variation factor(r/cf)	number of cycles(nt)	A0	A1, B1	A2, B2	A3, B3	Computation time (sec)
10	4	9.8	Not Compared			46.094
10	8	9.78	Not Compared			79.297
10	10	> 20	Not Compared			211
10	6	9.77	10.7,10.7	9.74,11.86	11.14,9.1	132.44
15	6	6.75	7.34,9.67	6.35,7.57	7.91,6.2	85.469
25	6	3.11	4.3,7.6	3.7,4.41	5,7	52.234
40	6	2.71	3.1,5.7	2.13,3.1	4.17,8.1	33.391
70	6	1.5	2.18,10.5	6.34,2.25	3.65,12.1	25.641
80	6	1.58	1.3,2.49	3.09,2.1	6.52,DNC	26.75
100	6	1.32	1.18,5.4	2.3,3.35	4.4,3.33	33.10
150	6	0.87	1.1,DNC	5,4	3.6,1.1	18.969
158	6	0.67	2.14,DNC	2.5,3.3	2.68,2.61	18

1. Estimated values of most important Fourier series coefficients converge towards actual values quicker as the rate of cuff pressure change is increased.
2. The fastest convergence of Fourier series coefficients is observed at r=158*cf which is a high gain controller. The pressure increases to 98.75 percent of maximum cuff pressure in one second.
3. Values above r=158*cf cause the system to start diverging significantly which results in an offset for the estimated blood pressure waveform when compared to true values. Divergence for r=158*cf is 0.72mmHg whereas for r=150*cf it is 0.426mmHg. Depending on the type of application, either of those may be acceptable whereas going to slower cuff pressure change rates is also an option. Although the divergence can be eliminated by increasing the number of cycles as they directly affect the final time and allow more time for the system to converge.

4. Computation time decreases significantly but this could be directly related to the quick convergence of estimated values.
5. At higher cuff pressure fluctuation rates, the less significant Fourier series coefficients do not converge to the actual values in many cases. Also, there are significant variations (up to even 40 times in some cases) in the starting duration where the estimated values vary rapidly before starting to settle down. These disturbances may cause for a misdiagnosis. However, the initial results can be discarded for a duration with threshold for differences caused due to changes in patients and environment.
6. The blood pressure waveform is accurately estimated even though some Fourier series coefficients do not converge to the actual values with increasing cuff pressure rates. Although the estimated values remain within a 5 percent error range even when they converge at a different value. In some cases, this makes it look like a system with higher rate of cuff pressure fluctuations converged slower. However, comparing the graphs always show that the estimate had stabilized earlier but towards a slightly different value.
7. On plotting the r/cf parameter on x-axis, and computation time on y-axis an exponential looking curve is obtained as shown in Figure 2.6.

2.3 Error and Covariance Testing

A Kalman filter is a linear dynamic system which works as an optimal estimator [52] for one or more variables using a given set of output measurements. An extended Kalman filter is used to estimate the states for a non-linear system and works by linearizing the system.

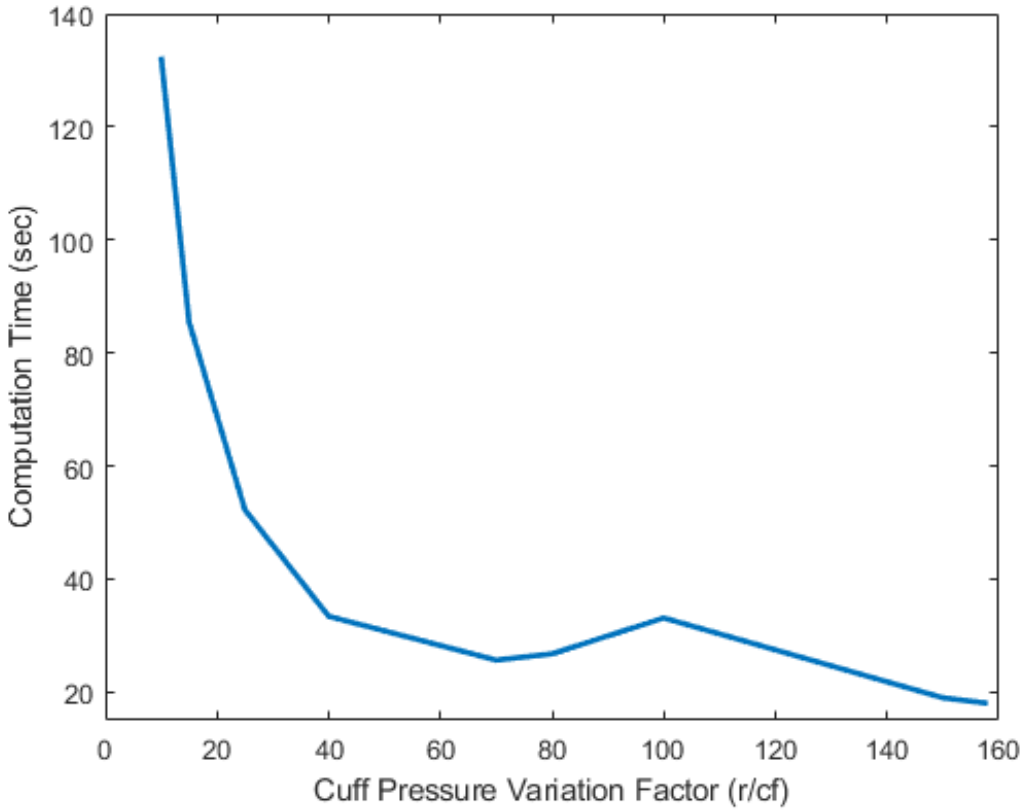

Figure 2.6. Cuff Pressure Variation Rate Vs. Computation Time.

2.3.1 System Operating within a Given Linear Region

In case the system is only operating within a range where the system mostly behaves linearly then the linearization can be done about that range. However, that is not the case with the system dynamics used for calculating the blood pressure waveform.

2.3.2 System Operating Over Larger Ranges or with High Fluctuations

As in this case, the system needs to be partially differentiated at each step. This is done by partially differentiating the A matrix with non-linear elements to get

a Jacobian so that the resulting matrix can be used as a system matrix [52]. This is explained using the equations below.

$$\dot{x} = a(x, u, t) + G(t)w, \tag{2.7}$$

$$z = h(x, t) + v, \tag{2.8}$$

$$A(x, t) = \frac{\partial a(x, u, t)}{\partial x}, \tag{2.9}$$

$$H(x, t) = \frac{\partial h(x, t)}{\partial x}, \tag{2.10}$$

Here, $\dot{x}$ is the derivative of state variables used to update the changes in variables through a given input u. In equation 2.7, $a(x, u, t)$ denotes a set of non-linear equations whereas w represents process noise which is considered to be negligible for our case. In equation 2.8, z represents the measured variables which are computed using the equations contained by $h(x, t)$ and are mainly dependent on the computed state variables. The dynamics are linearized by partially differentiating the set of non-linear equations in $a(x, u, t)$ and $h(x, t)$ to obtain Jacobians which replace A and H matrices which usually represent state (or system) matrix and output matrix respectively in case of linear systems. Equations 2.9 and 2.10 show the calculation of Jacobians for an extended Kalman filter operating in continuous time process.

In equation 2.8, the variable v represents the measurement noise whose covariance is specified using the R matrix in extended Kalman filter equations. This covariance value is altered to assess the amount of noise the filter can handle while functioning properly.

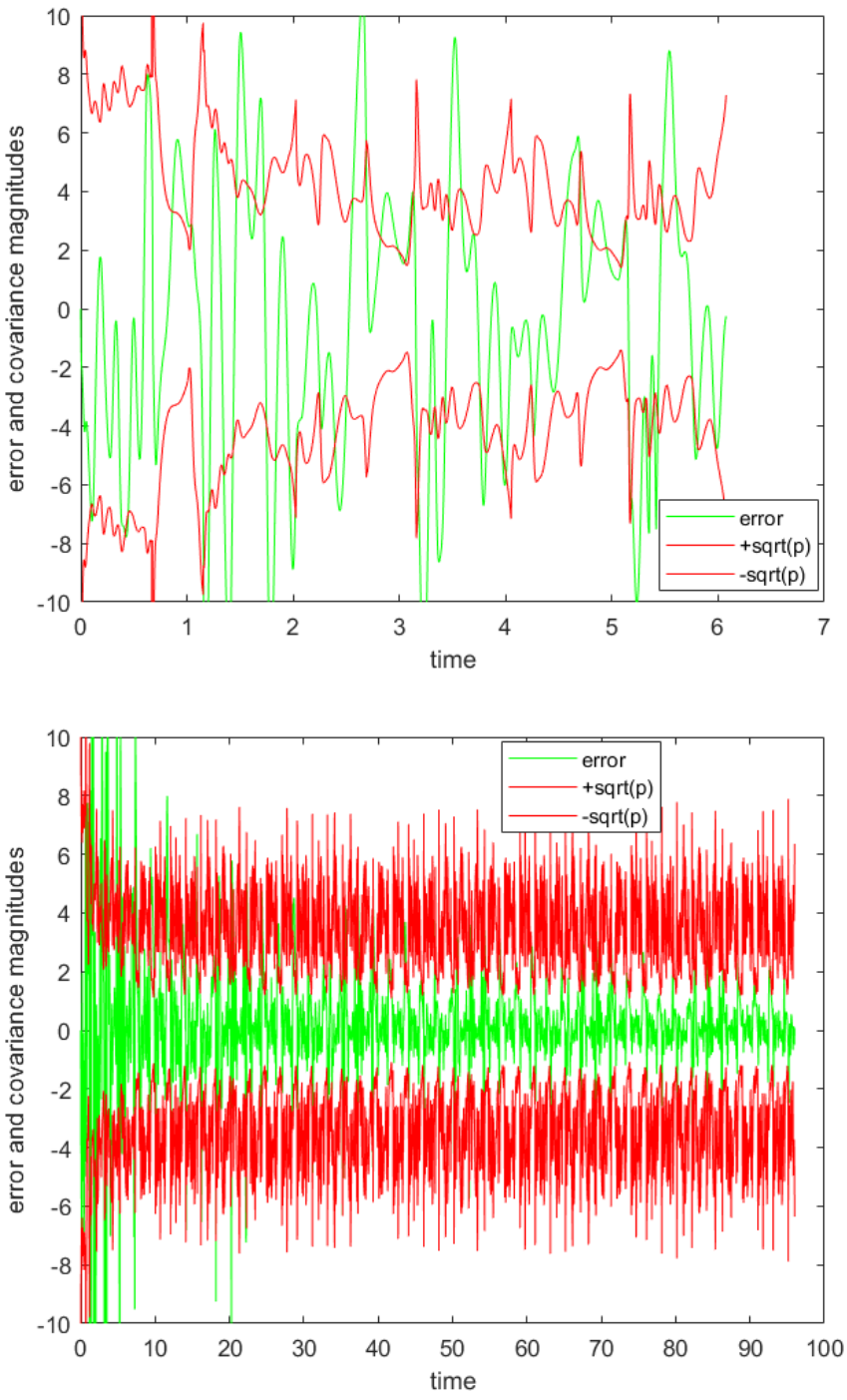

Figure 2.7. Error Vs. Covariance values for r=158*cf with different number of cycles (n = 6 and 90 respectively).

2.3.3 Analysis of Error and Covariance Values

The upper and lower thresholds for the noise determine the robustness of the estimator. Using different values, it was found that the upper limit for selecting initial measurement noise covariance matrix R is 1.0945 whereas the lower limit is 0.694. For R<0.694 the system is not able to converge so a stiff solver was tried using MATLAB command $ode15s$. This allowed for the system to converge with small divergences. Making the system dynamics continuous could help avert the divergence and allow for even lower initial R values which would improve the system further. A well-tuned Kalman filter has nearly 80 percent of error peaks within the covariance bounds. If all the peaks are above the covariance bounds then the filter is heavily depending on system model and neglecting the measurement values whereas all the values within the bounds indicate a filter that is neglecting the system model. The algorithm by Hullender and Brown is successfully able to fulfill these conditions for values or R ranging between 0.694 and 1.0945. This is true even for a high gain value of $r = 158 * cf$ and is shown in figure 2.7. Although, the number of cycles need to be increased sufficiently to allow the system to converge well. Other parameters affecting the error such as Q, X_o and P_o are not altered.

CHAPTER 3

EXTRACTING BLOOD PRESSURE WAVEFORM CHARACTERISTICS AND PREDICTING CARDIOVASCULAR DISEASES

In the previous section, it was confirmed that the estimate of blood pressure waveform provided by the algorithm developed by Hullender and Brown is accurate when operating within certain parameters of noise and cuff pressure change rates. Now, this section aims to develop an algorithm which can extract the important characteristics from the estimated blood pressure waveform and predict or diagnose some conditions based on standardized values. It should be noted that while the standardized values can accurately diagnose some diseases which are not affected by age, gender or other patient attributes, they might be a side effect of another disease or caused due to a scenario. For example, secondary hypertension has similar characteristics as hypertension but is caused by an underlying condition such as kidney disease, sleep apnea, thyroid issues etc. [53] Therefore, any diagnoses or information provided by the algorithm should be confirmed with a licensed medical professional before taking any medication or other steps to improve the cardiovascular health. The detailed code along with logic to implement the algorithm is presented in Appendix B.

3.1 Extracting Time Periods from the Blood Pressure Waveform

There are a number of time periods within the blood pressure waveform which can be used to assess the cardiovascular health by comparison to themselves or other time spans [54, 55]. One of the most important time periods is the cycle time which

represents the time duration of one complete blood pressure waveform cycle. Cycle time is necessary to measure the heart rate and is heavily linked to hypertension, atrial fibrillation and arrhythmia [13, 56, 57, 58]. While hypertension indicates sustained high blood pressures, atrial fibrillation relates to irregular heart rhythm and is termed as arrhythmia in case of very rapid heart rhythm [59, 60].

An algorithm is developed to determine cycle time by finding the duration between adjacent diastolic peaks as it iterates through systolic peaks. Since there is only one systolic peak during each cycle, this is a reliable method to determine cycle times accurately. The cycle time is monitored continuously, and output is provided in case the cycle time changes suddenly or abruptly. Studies show that unexpected changes in the cycle time can signal towards an upcoming or ongoing stroke, heart attack etc. [61, 62]

The final diagnostic report consists of the upper and lower thresholds for the cycle times along with the average and deviations. The deviations are highly useful to pinpoint anomalies during the measurement process. Any abnormal cycle times are noted to diagnose for atrial fibrillation and arrhythmia. Using standardized values, the algorithm also diagnoses tachycardia and bradycardia [63].

Furthermore, the algorithm also provides similar data regarding the systolic peak time, dicrotic notch and dicrotic peak periods. The MATLAB code to implement this algorithm is given in the final part of this chapter, the commented lines of code can be used to reliably implement the algorithm in other languages, without the use of inbuilt functions. This increases the versatility of algorithm so that it can be applied over different platforms with varying computational resources.

3.2 Evaluation of Cardiac Output Factors

The area under the blood pressure waveform is directly related to the volume of blood pumped by the heart. Although this volume can vary based on age, gender and body features, it can still provide important information and diagnose certain cardiovascular diseases simply by comparison of systolic and diastolic elements. The volume pumped by the heart within the systolic curve is known as the ventricular ejection or output [34]. This is a good way to assess if enough blood is reaching to the heart and can be used to diagnose coronary artery disease which is caused by a blockage or restriction in arteries leading to the heart [64, 65]. As per experimental research, this condition usually results in low stroke volume output despite high systolic pressure especially during exercise. The cardiac output factor combined with the ratio of systolic duration to cycle time is a reliable measure to diagnose the severity of coronary artery disease [66, 67].

Furthermore, comparison of the ventricular output to the entire area under the curve and/or the area under the diastolic region can also provide useful information to measure cardiovascular health [33, 35]. Among other conditions which can be diagnosed by comparing cardiac output factors, the most important ones are arterial sclerosis which refers to the hardening of arteries, and stroke occurrence [68].

The algorithm is extended to calculate the area under the systolic and diastolic regions of the blood pressure waveform curve. It then compares the time for ventricular output to the total cycle time. These are good indicators of arterial sclerosis as confirmed by Meune and Lambova in independent research [69, 70].

The algorithm also monitors the mean and deviations from the cardiac output factors to notice sudden changes which can point towards arrhythmia or even a heart attack [71]. This is especially crucial to accurately diagnose silent heart attacks immediately and take necessary measures to mitigate further damage to the heart.

Comparing ventricular output factor for different activity modes (rest, exercise) allows prediction of heart attacks, strokes and other risks [72, 73]. This also helps in remotely monitoring patients and determining situations or environments which can lead to abnormal heart activity when compared to normal values [74].

3.3 Shape of the Blood Pressure Waveform Curve

The slope for pressure increases during systolic peak and the depth of the dicrotic notch also referred to as incisura are important factors of blood pressure waveform [75, 76]. These factors can be reliably used to predict the artery thickness, artery blockage, atrial valve function and other parameters important for assessment of cardiovascular health. A comparison and continuous assessment of these parameters can be used for accurately diagnosing major cardiovascular diseases including arterial sclerosis, aortic stenosis, aortic regurgitation, hypertrophic obstructive cardiomyopathy, coronary artery disease, atrial fibrillation and stroke [19, 77].

3.3.1 Assessment of Dicrotic Notch

When the aortic valve within the heart narrows abnormally, the condition is termed as aortic stenosis. According to many studies, this condition can be predicted by a small depth of dicrotic notch or an indistinct incisura [78, 76, 36].

3.3.2 Assessment of Systolic Peak Slopes

In case of hypertrophic obstructive cardiomyopathy, where the muscle of the heart becomes thick in an abnormal manner making it hard for the heart to pump blood. As explained by Yartsev and Mark in their respective books, on the blood pressure waveform, this is seen by a splitting of the systolic peak into two parts with a steep decline after the first systolic peak.

When the heart valve does not close properly, it leads to a back flow of blood into the heart. This condition is termed as aortic regurgitation. On the blood pressure waveform curve, this is signified by a steep decline after the systolic peak followed by an indistinct incisura [79, 36].

3.3.3 Algorithm to Assess Blood Pressure Waveform's Shape

The algorithm calculates the slope of the systolic pressure rise from the previous diastolic peak to the systolic peak. Many sources segregate this slope at the anacrotic notch to segregate forward wave and reflected wave. However, the anacrotic notch is usually indistinct in normal blood pressure waveforms and the estimation algorithm developed by Hullender and Brown provides a smooth curve with no anacrotic notch. Following the peak, the algorithm calculates the slope from the systolic peak to the dicrotic notch.

The depth for dicrotic notch is calculated in terms of mmHg by comparing the pressures at dicrotic notch and dicrotic peak. The depth of dicrotic notch is an important parameter to assess artery thickness [80, 81] and proper closing of valves. The average and deviation for these values are also calculated to assess any abnormal changes [54].

3.4 Blood Pressure Analysis

Although measuring blood pressure is common, the blood pressure waveform provides much more detailed information regarding the blood pressures [82, 10, 30]. Instead of just two peaks, an algorithm is developed which monitors the blood pressure peaks constantly. These can be effectively used to assess important cardiovascular diseases such as hypertension and its severity [83, 84], risk of coronary artery disease and possibility of cardiovascular incidents [85, 86]. As per a 1986 study by Berthe,

a medical professional may be able to determine the severity and even location of coronary artery disease when there is an abnormal change in blood pressure levels after a specific physical activity [87]. Similarly, the fluctuations observed with different activities can be used to assess the cardiovascular risk for a patient [88].

The algorithm determines the systolic and diastolic pressure then compares them to standardized values for diagnosing the severity of elevated or low blood pressure and hypertensive stages [89]. Additionally, it constantly evaluates the total time and compares it to the time with elevated blood pressure. According to a 2002 study published in the American Heart Association, this helps in diagnosing the hypertension severity [90]. Average, thresholds and deviation for both systolic and diastolic pressure are provided in the diagnostic report so that a medical professional can pinpoint the anomalies.

3.5 Factors to Consider While Analyzing the Diagnostic Report

The report provided by the algorithm provides some information which needs to be compared to other data such as the cardiac output factors. Moreover, various assumptions are made by Hullender and Brown while modeling the system and developing the algorithm; even more assumptions are made while developing the algorithm which might not be true in the real world. For example, the baseline pressure of the body keeps changing as the body tries to regulate the internal body pressures, these changes in baseline pressure depend on posture, environment and activity level of the patient along with other things [91, 92]. Another example would be the absence of process noise within the extended Kalman Filter algorithm developed by Hullender and Brown. The process noise can occur due to fluctuations in the functioning of pressure transducers, or changes in the body due to internally reflected pressure waves or environment among other things.

3.6 Limitations of the algorithm

The algorithm shares the same limitations as the extended Kalman filter since it does not improve or alter the estimates in any way. Furthermore, the algorithm would not able to function properly if there are additional peaks due to an underlying medical condition.

Due to varying medical studies and changes in technology, there is conflicting data when trying to diagnose or predict a cardiovascular disease in many instances. For example, a 1961 study by Buteler concluded that systolic upstroke time is not a reliable measure for aortic stenosis [93] although many sources claim them to be linked directly [94, 95]. Therefore, further studies with more patients need to be conducted before a characteristic of the blood pressure waveform is used for diagnosis.

CHAPTER 4

RESULT AND DISCUSSION

The rate of cuff pressure change at a high gain of 0.98 times the maximum pressure allows for the quickest convergence without significant deviation. The deviations can be reduced by increasing the number of cycles which allows the system to converge closer to the actual values.

Higher gains allow a greater number of cuff pressure cycles to be completed in shorter amount of time. They also result in increased cuff pressure variations to provide more input data to the algorithm developed by Hullender and Brown. These factors result in a lower computation time. A combination of high gain and ample number of cycles can be implemented to obtain reliable estimates for any given application.

The rates of cuff pressure change beyond $158 * cf$ cause significant divergence from estimates which may be removed by increasing the number of cycles. However, this will further increase the computation time and might not be desirable as increasing the number of cycles increases the computational requirements.

Over the tested ranges in table 2.2, the convergence time decreases in an exponential manner as the rate of cuff pressure variation is increased.

The algorithm functions effectively and is able to reliably extract the important characteristics from the blood pressure waveform. An alternative code is included as a commented section (shown in Chapter 3), which can be used to implement the algorithm without using MATLAB functions. This allows the algorithm to be directly implemented in other languages such as Python, C and C++ which can be supported by a wide range of devices and platforms.

After assessing the blood pressure levels, cycle times and other parameters along with their changes, the algorithm diagnoses for the following cardiovascular diseases by comparing them to standardized values:

1. Blood pressure level along with hypertension severity
2. Arrhythmia
3. Atrial Fibrillation
4. Tachycardia and Bradycardia

The algorithm displays all the parameters along with their variations in the final diagnostics report output. If any anomalies or sudden changes are noticed, then they can be clearly seen in the report through the standard deviation metrics.

A sample output of the diagnostic report printed by the algorithm in MATLAB is included in Appendix B.

It is seen from the report that the algorithm is able to accurately diagnose cardiovascular diseases and extract all the required characteristics. The algorithm has also been modified further to ignore the first 10 cycles as the extended Kalman filter needs some time to converge to the real values. Finally, the thresholds can be changed as required to better diagnose the cardiovascular anomalies.

CHAPTER 5

FUTURE WORK

As described by Dr. Hullender, the existing algorithm can be expanded by continuation of the equations within the system model to accommodate wider ranges of initial measurement noise value, R. Furthermore, advanced computation techniques such as machine learning and neural networks can be used to relate different factors such as age, gender and physical characteristics with multiple features extracted from the blood pressure waveform.

Additional algorithm can be added before the existing algorithm to readjust the estimated blood pressure waveform or account for changes related to:

1. Natural and continuous events such as baseline fluctuations [31]
2. Presence of a cardiovascular disease such as hemodynamic instability [96]
3. Patient to patient variations due to age [97], gender and physical characteristics [91] among other things.

In terms of practical devices, a portable cuff-type pressure transducer type device can be used to assess blood pressure remotely at any time of the day by connecting it to mobile devices like smartphones, tablets and laptops.

APPENDIX A

ALGORITHM AND CODE TO EXTRACT AND ANALYZE BLOOD PRESSURE WAVEFORM CHARACTERISTICS

In the following appendix, the code is presented along with the algorithms used to develop the logic for the program. This program is developed for MATLAB but an additional section is included using which the program can be implemented in any modern language such as C++, Python etc.

Throughout the code, comments have been used to explain the steps taken. These comments start with a % symbol whereas the sections for MATLAB specific and general code are spli using two %% symbols together.

```
%% Algorithm to Analyze the Blood Pressure Waveform
%To calculate computational time, a variable is initialized in the first
%line to store CPU time and a variable is initialized in the last line to
%substract the current CPU time from the initial CPU time. Both lines of
%code are given below as comments respectively.

%tstart=cputime
%tend=cputime-tstart

%The algorithm only needs the estimated blood pressure waveform for
%analysis and thus it can be included within the model developed by
%Hullender and Brown or as a separate function which only fetches the
%estimated blood pressure waveform values.

%initializing variables to recognize anomalies
SElevBp=0;
SHighBpStage1=0;
SHighBpStage2=0;
SHypertensiveCrisis=0;
```

```
SLowBp=0;
DHighBpStage1=0;
DHighBpStage2=0;
DHypertensiveCrisis=0;
DLowBp=0;
tnow=0;
tfor=0;
rangeCycle=0;
cyclenum=0;
Fib=0;
slf=0;
cyclen2=0;
COf=0;
TachyCar=0;
BradyCar=0;
ArrhythmiaSt=0;
ElevBPDur=0;

%% Section - 1: To Run Code Without MATLAB findpeaks functions
%all other functions used are common and can be coded easily
%across different languages although similar functions may already exist
%under a different name depending on the programming language and library

% JD=PE/cf;
% negJD=-JD;
% duo=0;
```

```
% for numit=1:1:length(JD)-2
%
% % conditional statement to find peaks
%   if (JD(numit+1)-JD(numit)>0) &&  (JD(numit+2)-JD(numit+1) <= 0)
%       duo=duo+1;
%       PeakMag(duo)=JD(numit+1);
%       Locats(duo)=t(numit+1);
%   end
% %conditional statement to find trough/valleys
%   if (negJD(numit+1)-negJD(numit)>0) && (negJD(numit+2)-negJD(numit+1)<=0)
%       LowPeaks(duo)=-negJD(numit+1);
%       LowLocats(duo)=t(numit+1);
%   end
% end

%% Section - 2: Code using MATLAB Functions

%to run the code without errors due to multiple assignments, only one
%section should be run and other commented

%fetching peak values and their time locations
JD=PE/cf; %PE is the estimated blood pressure waveform
[PKs,LOCs,wi,pr]=findpeaks(JD,t,'WidthReference','halfheight'); %peaks
PeakMag=PKs; %magnitude of peaks
Locats=LOCs; %time locations of peaks
SysPeakWidth=wi;
```

```
%fetching minimum trough/valley magnitudes and their time locations
[BPKs,BLOCs,Bwi,Bpr]=findpeaks(-JD,t); %valleys
LowPeaks=-BPKs; %magnitude of valleys
LowLocats=BLOCs; %time locations of valleys
systamp=zeros(1,floor(length(PeakMag)/3));

%% Algorithms below use basic functions
%NOTE - It is assumed that the system needs the time for first 10 peaks to
%converge to the actual values of blood pressure waveform. Therefore, the
%first 10 peaks are neglected throughout the algorithm when evaluating the
%estimated blood pressure waveform.


%iterating through systolic peaks
for iter=11:1:floor((length(PeakMag)-2)/3)
    if PeakMag(iter)>PeakMag(iter+1) && PeakMag(iter)>PeakMag(iter+2)
    SysP(iter)=PeakMag(3*iter-2);
    DiaP(iter)=LowPeaks(3*iter);
    end
end

%Average, maximum, mimimum and standard deviation of systolic pressure
AverageSystolicPressure=mean(SysP);
MaxSysP=max(SysP);
MinSysP=min(SysP);
```

```
DevSysP=std(SysP);

%Average, maximum, mimimum and standard deviation of diastolic pressure
ADiaP=mean(DiaP);
MaxDiaP=max(DiaP);
MinDiaP=min(DiaP);
DevDiaP=std(DiaP);



%recognizing anomalies in systolic pressure
for isy=11:1:(length(PeakMag)-3)
    if abs(PeakMag(isy)-PeakMag(isy+3))>5
        Fib=1;
    end
%classifying hypertension/high BP severity based on systolic pressure
    if PeakMag(isy)>PeakMag(isy+1) && PeakMag(isy)>PeakMag(isy+2)
        if  PeakMag(isy)>=120 && PeakMag(isy)<130
            SElevBp=1;
        elseif PeakMag(isy)>=130 && PeakMag(isy)<140
            SHighBpStage1=1;
        elseif PeakMag(isy)>=140 && PeakMag(isy)<180
            SHighBPStage2=1;
        elseif PeakMag(isy)>=180
            SHypertensiveCrisis=1;
        elseif PeakMag(isy)<90
            SLowBp=1;
```

```
        end
        cyclenum=cyclenum+11;

%calculating cycle time
        rangeCycle(cyclenum)=Locats(isy+3)-Locats(isy);
        if isy>3
            slf=slf+1;

%calculating slope to reach systolic pressure
            SysSlope(slf)=floor((PeakMag(isy)-LowPeaks(isy-1))/...
                (Locats(isy)-LowLocats(isy-1)));

%calculating slope after the systolic pressure
            SystolicDecrementSlope(slf)=floor((PeakMag(isy)...
            -LowPeaks(isy))/(Locats(isy)-LowLocats(isy)));

%calculating dicrotic notch depth
            DicNotchDepth(slf)=floor(PeakMag(isy+1)-LowPeaks(isy));

%calculating duration of elevated blood pressure
            if PeakMag(isy)>120 || LowPeaks(isy-1)>80
                ElevBPDur=ElevBPDur+rangeCycle(cyclenum);
            end
        end

%diagnosing intermittent arrhythmia based on fluctuation in cycle time
```

```
%The thresholds can vary depending on patient's age, gender etc.
        if cyclenum>10
            prevCycle(cyclenum)=rangeCycle(cyclenum-1);
            if prevCycle(cyclenum)>1.2*rangeCycle(cyclenum)...
                    || prevCycle(cyclenum)<0.8*rangeCycle(cyclenum)
                ArrhythmiaSt=1;
            end

%diagnosing Tachycardia and Bradycardia
            if rangeCycle(cyclenum)<0.6
                TachyCar=1;
            elseif rangeCycle(cyclenum)>1
                BradyCar=1;
            end
        end
     end
end

%determining average and deviations for slope to reach systolic pressure
AvSysSlope=mean(SysSlope);
DevSysSlope=std(SysSlope);

%determining average and deviations for dicrotic notch depth
AvDicND=mean(DicNotchDepth);
DevDicND=std(DicNotchDepth);
```

```
%determining average and deviations for slope after systolic pressure
AverageSystolicDecrementSlope=mean(SystolicDecrementSlope);
DeviationSystolicDecrementSlope=std(SystolicDecrementSlope);

%determining the ratio of high blood pressure cycles to normal ones
%this helps in determining if the elevated blood pressures are constant
TotalTime=sum(rangeCycle);
ElevBPDuration=sum(ElevBPDur);
RatioElevBP=ElevBPDuration/TotalTime;

%determining maximum, miminum, average and deviations in cycle time
MaxCyc=max(rangeCycle);
AvgCyc=mean(rangeCycle);
BeatDev=std(rangeCycle);
MinCyc=min(rangeCycle);

%recognizing anomalies in diastolic pressure
for kdi=11:1:(length(LowPeaks)-3)

%classifying hypertension/high BP severity based on diastolic pressure
    if LowPeaks(kdi)<LowPeaks(kdi+1) && LowPeaks(kdi+1)>LowPeaks(kdi+2)
        if LowPeaks(kdi)>=80 && LowPeaks(kdi)<90
            DHighBpStage1=1;
        elseif LowPeaks(kdi)>=90
            DHighBpStage2=1;
        elseif LowPeaks(kdi)>=120
```

```
            DHypertensiveCrisis=1;
        elseif LowPeaks(kdi)<60
            DLowBp=1;
        end

%evaluating other time periods for comparison
        for kco=1:1:length(t)
            if LowLocats(kdi)==t(kco)
                tnow=kco;
            end
        end

%evaluating ventricular output factor and duration
        for kco2=1:1:length(t)
            if LowLocats(kdi+1)==t(kco2)
                tfor=kco2;
                if tnow>=1
                    cyclen2=cyclen2+1;
                    curWave=JD(tnow:tfor);
                    rangeSys=t(tnow:tfor);
                    COf=COf+1;
                    VentricularOutDur(COf)=LowLocats(kdi+1)-LowLocats(kdi);
                    SysCOfactor(COf)=trapz(rangeSys,curWave);

%evaluating durations to reach systolic peak and dicrotic peak
                    DicPeakDur(COf)=Locats(kdi+2)-LowLocats(kdi);
```

```
                    SysPeakDur(COf)=Locats(kdi+1)-LowLocats(kdi);

%calculating the ratio of systolic duration/time to reach dicrotic notch
%to overall cycle
                    sysRatio(COf)=(t(tfor)-t(tnow))/rangeCycle(cyclen2);
                end
            end

%calculating diastolic cardiac output factor i.e., area under the diastolic
%curve
            if LowLocats(kdi+3)==t(kco2)
                tnxt=kco2;
                if tnow>=1
                    diaWave=JD(tfor:tnxt);
                    rangeDia=t(tfor:tnxt);
                    DiaCOfactor(COf)=trapz(rangeDia,diaWave);
                end
            end
        end
    end
end

%evaluating the average and deviations in systolic and diastolic
%cardiac output factors
MeanSyCO=mean(SysCOfactor);
MeanDiaCO=mean(DiaCOfactor);
```

```
DevSyCO=std(SysCOfactor);
DevDiaCO=std(DiaCOfactor);

%evaluating average and deviations in systolic ratio to cycle time
MeanSysRatio=mean(sysRatio);
DevSysRatio=std(sysRatio);

%average and deviations in ventricular output duration
AvgVentOutDur=mean(VentricularOutDur);
DevVentOutDur=std(VentricularOutDur);

%average and deviations in duration to reach systolic peak
AvgSystolicPeakDuration=mean(SysPeakDur);
DevSystolicPeakDuration=std(SysPeakDur);

%average and deviations in duration to reach dicrotic peak
AvgDicroticPeakDuration=mean(DicPeakDur);
DevDicroticPeakDuration=std(DicPeakDur);

%Diagnostic Report with important characteristics and diagnoses
CycStr=['\n\n Patient Diagnostic Report \n\nNote: 0 indicates ' ...
    'a negative result and 1 indicates a positive result.' ...
    '\nAll durations are in seconds. \n\nMaximum Cycle Time = %.2f'...
    '\nAverage Cycle Time = %.2f \nDeviation in Cycle Time = %.2f'...
    '\nMinimum Cycle Time = %.2f'];
fprintf(CycStr,MaxCyc,AvgCyc,BeatDev,MinCyc)
```

```
TimePerStr=['\n\nAverage Time to Reach Systolic Peak = %.2f'...
    '\nDeviation in Time to Reach Systolic Peak = %.2f'...
    '\n\nAverage Time to Reach Dicrotic Peak = %.2f'...
    '\nDeviation in Time to Reach Dicrotic Peak = %.2f'...
    '\n\nAverage Ventricular Output Duration = %.2f'...
    '\nDeviation in Ventricular Output Duration = %.2f'];
fprintf(TimePerStr,AvgSystolicPeakDuration,DevSystolicPeakDuration,...
    AvgDicroticPeakDuration,DevDicroticPeakDuration,AvgVentOutDur,...
    DevVentOutDur)

ShapeStr=['\n\nAverage Slope to reach Systolic Peak = %.2f mmHg/sec'...
    '\nDeviation in Slope to reach Systolic Peak = %.2f \n\nAverage'];
fprintf(ShapeStr,AvSysSlope,DevSysSlope)

SystolicDecrementString=['\n\n Average Slope after the Systolic Peak'...
    ' = %.2f \n Deviation in Slope after the Systolic Peak = %.2f'...
    '\n\nAverage Dicrotic Notch Depth = %.2f mmHg \nDeviation in Dicrotic'...
    'Notch Depth = %.2f'];
fprintf(SystolicDecrementString,AverageSystolicDecrementSlope,...
    DeviationSystolicDecrementSlope,AvDicND,DevDicND)

TimeDurStr=['\n\nTotal Time Monitored = %.2f \nDuration of Elevated'...
    'Blood Pressure = %.2f \nRatio of Elevated Blood Pressure'...
    'to Total Time = %.2f'];
fprintf(TimeDurStr,TotalTime,ElevBPDuration,RatioElevBP)
```

```
VentrStr=['\n\nMean Ventricular Output Factor = %.2f'...
    '\nDeviation in Ventricular Output Factor = %.2f'];
fprintf(VentrStr,MeanSyCO,DevSyCO)

DiastStr=['\nMean Diastolic Output Factor = %.2f'...
    '\nDeviation in Diastolic Output Factor = %.2f'];
fprintf(DiastStr,MeanDiaCO,DevDiaCO)

PeriodComparisonStr=['\n\nMean Ratio of Systolic Duration to Total'...
    'Cycle Duration = %.2f \nDeviation in Ratio of Systolic'...
    'Duration to Total Cycle Duration = %.2f'];
fprintf(PeriodComparisonStr,MeanSysRatio,DevSysRatio)

SysPAStr=['\n\nAverage Systolic Pressure %.2f mmHg'...
    '\nMaximum Systolic Pressure %.2f mmHg'...
    '\nMinimum Systolic Pressure %.2fmmHg'...
    '\nStandard Deviation in Systolic Pressure'...
    '%.2f mmHg'];
fprintf(SysPAStr, AverageSystolicPressure, MaxSysP, MinSysP, DevSysP)

DiaPAStr=['\n\n Average Diastolic Pressure = %.2f mmHg'...
    '\nMaximum Diastolic Pressure = %.2f mmHg'...
    '\nMinimum Diastolic Pressure = %.2f mmHg'...
    '\nStandard Deviation in Diastolic Pressure = %.2f mmHg'];
fprintf(DiaPAStr,ADiaP, MaxDiaP, MinDiaP, DevDiaP)
```

```
fprintf('\n \nAtrial Fibrilation - %d',Fib)

DiagATBStr=['\nArrythmia - %d \nTachycardia (Elevated Heartbeat)'...
    '- %d \nBradycardia (Slow Heartbeat) - %d \n\n'];
fprintf(DiagATBStr,ArrhythmiaSt,TachyCar,BradyCar)

%combining systolic and diastolic anomalies to diagnose blood pressure and
%hypertension severity
if SHypertensiveCrisis==1 || DHypertensiveCrisis==1
    fprintf('Hypertensive crisis!')
elseif SHighBPStage2==1 || DHighBpStage2==1
    fprintf('High Blood Pressure - Stage 2')
elseif SHighBpStage1==1 || DHighBpStage1==1
    fprintf('High Blood Pressure - Stage 1')
elseif SElevBp==1
    fprintf('Elevated Blood Pressure')
elseif SLowBp==1 || DLowBp==1
    fprintf('Low Blood Pressure')
else
    fprintf('Blood Pressure is normal')
end
fprintf('\nEnd of Report.\n')
```

APPENDIX B

SAMPLE OF THE GENERATED DIAGNOSTIC REPORT

This appendix shows a sample output diagnostic report generated by the code in Appendix A.

```
Patient Diagnostic Report

Note: 0 indicates a negative result and 1 indicates a positive result.
All durations are in seconds.

Maximum Cycle Time = 1.01
Average Cycle Time = 1.00
Deviation in Cycle Time = 0.00
Minimum Cycle Time = 0.99

Average Time to Reach Systolic Peak = 0.27
Deviation in Time to Reach Systolic Peak = 0.00

Average Time to Reach Dicrotic Peak = 0.61
Deviation in Time to Reach Dicrotic Peak = 0.00

Average Ventricular Output Duration = 0.44
Deviation in Ventricular Output Duration = 0.00

Average Slope to reach Systolic Peak = 267.13 mmHg/sec
Deviation in Slope to reach Systolic Peak = 2.84

Average Slope after the Systolic Peak = -327.96
Deviation in Slope after the Systolic Peak = 4.94
```

Average Dicrotic Notch Depth = 11.00 mmHg

Deviation in DicroticNotch Depth = 0.00

Total Time Monitored = 95.00

Duration of ElevatedBlood Pressure = 94.00

Ratio of Elevated Blood Pressureto Total Time = 0.99

Mean Ventricular Output Factor = 54.38

Deviation in Ventricular Output Factor = 0.28

Mean Diastolic Output Factor = 56.94

Deviation in Diastolic Output Factor = 0.26

Mean Ratio of Systolic Duration to TotalCycle Duration = 0.44

Deviation in Ratio of SystolicDuration to Total Cycle Duration = 0.00

Average Systolic Pressure 54.63 mmHg

Maximum Systolic Pressure 160.49 mmHg

Minimum Systolic Pressure 0.00mmHg

Standard Deviation in Systolic Pressure76.45 mmHg

Average Diastolic Pressure = 30.30 mmHg

Maximum Diastolic Pressure = 89.08 mmHg

Minimum Diastolic Pressure = 0.00 mmHg

Standard Deviation in Diastolic Pressure = 42.41 mmHg

Atrial Fibrilation - 0

Arrythmia - 0

Tachycardia (Elevated Heartbeat)- 0

Bradycardia (Slow Heartbeat) - 1

High Blood Pressure - Stage 2

End of Report.

APPENDIX C

HULLENDER AND BROWN'S WAVEFORM ESTIMATION ALGORITHM

This appendix explains the algorithm developed by Hullender and Brown along with the techniques used within it such as Fourier transform and the extended Kalman filter.

Hullender and Brown modeled a cuff pressure oscilloscope system where blood pressure is measured by placing a cuff around the arm of the patient then raising the cuff pressure $P_c(t)$ to maximum before reducing it back to zero in cycles by changing the cuff volume $V_c(t)$. The changing cuff pressure and internal blood flow cause volume changes in artery which sends small disturbances to the cuff. The model of the system developed by Hullender [19] measures these disturbances and then estimates the blood pressure waveform along with the stiffness of the wall arteries. The model formation approach uses mathematical formulae for fluid flow and nonlinear estimation using an extended Kalman Filter. The equations used to define the system are given below:

$$V_c\ (t) = V_o\ e^{\frac{-5P_c\ (t)}{P_{cm}}} + V_{cm}\ (1 - e^{\frac{-5P_c\ (t)}{P_{cm}}}), \tag{C.1}$$

in the above equation, V_o and V_{cm} represent the initial and maximum cuff volumes whereas P_{cm} refers to the maximum cuff pressure. Next, the equation relating cuff volume change $\dot{V}_c\ (t)$ to the derivative of cuff pressure oscillations $\dot{y}\ (t)$ and transmural pressure P_t such that $P_t(t) = P(t) - P_c(t)$.

$$\dot{y}\ (t) = \frac{1.4P_{ca}}{V_c(t)}\ \dot{P}_t(t)V_{ao}\ f(P_t), \tag{C.2}$$

where P_{ca} refers to the absolute cuff pressure, V_{ao} signifies the artery volume when $P(t) = P_c(t)$ making the transmural pressure $P_t(t) = 0$. $f(P_t)$ refers to the compliance function for artery walls.

$$f(P_t) = ae^{-bP_t} \quad for \quad P_t(t) \geq 0, \tag{C.3}$$

$$f(P_t) = ae^{-aP_t} \quad for \quad P_t(t) \leq 0, \tag{C.4}$$

where a and b are constants. The slope of the compliance function directly relates to the arterial stiffness. A smaller slope would require higher change in transmural pressure to change the volume by a certain amount which means that the artery walls are stiffer [98]. Equations were verified once again to check for accuracy using adiabatic capacitance equations for fluid systems [99, 100, 50]. Furthermore, the extended Kalman filter was also assessed to gain a deeper understanding of the estimated waveform [52].

C.1 Fourier series formation

For this research, the blood pressure waveform is assumed to be repeating at a fixed frequency with similar amplitudes under normal health circumstances which makes it a periodic function [101]. However, it should be noted that the real blood pressure waveform is neither constant in frequency nor amplitude. The frequency can change depending on the body activity, mental state and environmental factors among others. Furthermore, the amplitudes for blood pressure waveform can often change due to the baseline offset. In order to regulate the internal body pressures, the mean blood pressure keeps changing which is referred to as baseline offset. It is possible to remove these disturbances from the blood pressure waveform using filtering methods. Therefore, the model can be extended using existing research to overcome normal fluctuations in frequency and amplitude which would make it feasible for practical applications in future.

A periodic function can be estimated using a combination of sine and cosine wave elements. More elements allow for a better fit between estimated and actual function and a series with infinite elements also known as Fourier series can be used

to replicate any periodic function. To estimate the blood pressure waveform, it is converted to a Fourier series with 11 elements.

$$P(t) = A_o + A_1 sin(\omega t) + A_2 sin(2\omega t) + A_3 sin(3\omega t) + A_4 sin(4\omega t) \\ + B_1 cos(\omega t) + B_2 cos(2\omega t) + B_3 cos(3\omega t) + B_4 cos(4\omega t) + B_5 cos(5\omega t), \tag{C.5}$$

where A_i and B_i represent the amplitudes of sine and cosine elements while ω represents the unknown frequency. The values for coefficients representing amplitudes for sine and cosine waves are recalculated using Fourier series equations and it is verified that the coefficients taken are correct.

C.2 Extended Kalman Filter Functioning

A Kalman filter is an optimal estimation algorithm that functions in two steps known as prediction and correction. During the first step of prediction, it estimates the states based on input and using previous data. In the correction or update step it uses the output values measured for the same input and then compares them to the estimated values for updating the prediction and estimated state matrix using weighted averages also known as Kalman gain [52, 102]. While the algorithm is a recursive algorithm, it can also work in real time by only using the current input, uncertainty matrices and previously estimated states.

Kalman filter is also termed as linear quadratic estimator and can only work with linear systems. However, since most systems are non-linear in nature, extensions for Kalman filter are developed to accurately estimate the states. The model developed by Hullender and Brown uses an extended Kalman filter which functions by partially differentiating the non-linear equations at each step. In cases where the system only operates over a given approximately linear range then the system dynamics can be partially differentiated over that range to get accurate estimates.

In the original model, the simulation is run for a total of 96 seconds allowing for 3 cycles of cuff pressure increment till 160mmHg and reduction to zero at the rate of 10mmHg/sec. A total of 16 parameters are estimated which include the 11 Fourier coefficients, frequency of blood pressure waveform cycle (ω), artery volume (V_{ao}) at zero transmural pressure ($P_t(t)$=0), cuff pressure fluctuations ($y(t)$) and arterial compliance constants denoted by a and b.

REFERENCES

[1] W. H. Organization. (2020, Dec.) The top 10 causes of death. [Online]. Available: https://www.who.int/news-room/fact-sheets/detail/the-top10-causes-of-death

[2] K. D. Kochanek, J. Xu, and E. Arias, "Mortality in the united states, 2019," NCHS Data Brief, no. 395, Dec. 2020. [Online]. Available: https://www.cdc.gov/nchs/data/databriefs/db395-H.pdf

[3] F. B. Ahmad, J. A. Cisewski, A. Minin˜o, and R. N. Anderson, "Provisional mortality data — united states, 2020," MMWR Morb Mortal Wkly, vol. 70, pp. 519–522, 2021.

[4] W. H. Organization. (2021, June) Cardiovascular diseases (cvds). [Online]. Available: https://www.who.int/news-room/fact-sheets/detail/cardiovasculardiseases-(cvds)

[5] C. D. Fryar, T. C. Chen, and X. Li, "Prevalence of uncontrolled risk factors for cardiovascular disease: United states, 1999–2010," NCHS data brief., no. 103, 2012. [Online]. Available: https://www.cdc.gov/nchs/data/databriefs/db103.pdf

[6] A. H. Association. (2015, July) Silent ischemia and ischemic heart disease. [Online]. Available: https://www.heart.org/en/health-topics/heartattack/about-heart-attacks/silent-ischemia-and-ischemic-heart-disease

[7] U. D. of Health, C. f. D. C. Human Services, and Preventions. National diabetes statistics report, 2020. [Online]. Available: https://www.cdc.gov/diabetes/pdfs/data/statistics/national-diabetesstatistics-report.pdf

[8] A. K. Fund. Heart disease chronic kidney disease (ckd). [Online]. Available: https://www.kidneyfund.org/kidney-disease/chronic-kidneydisease-ckd/complications/heart-disease/

[9] H. Pandey and S. Prabha, "Smart health monitoring system using iot and machine learning techniques," pp. 1–4, 2020.

[10] N. Raheja and A. K. Manoacha, A Study of Telecardiology-Based Methods for Detection of Cardiovascular Diseases, S. Jain and S. Paul, Eds. Singapore: Springer Singapore, 2020. [Online]. Available: https://doi.org/10.1007/978981-15-2740-112

[11] H.-K. Ra, J. Ahn, H. J. Yoon, J. Ko, and S. H. Son, “Accurately measuring heartrate using smart watch,” pp. 100–100, 2016.

[12] K. Wasilewska and J. Rumin´ski, “Analysis of the accuracy of pulse estimation using smart watches,” pp. 519–525, 2018.

[13] S. K. Jain and B. Bhaumik, “An energy efficient ecg signal processor detecting cardiovascular diseases on smartphone,” IEEE Transactions on Biomedical Circuits and Systems, vol. 11, no. 2, pp. 314–323, 2017.

[14] B. Mishra, N. Arora, and Y. Vora, “An ecg-ppg wearable device for real time detection of various arrhythmic cardiovascular diseases,” pp. 1–5, 2019.

[15] M. Aboy, J. McNames, T. Thong, D. Tsunami, M. Ellenby, and B. Goldstein, “An automatic beat detection algorithm for pressure signals,” IEEE Transactions on Biomedical Engineering, vol. 52, no. 10, pp. 1662–1670, 2005.

[16] J. Seo, S. J. Pietrangelo, H.-S. Lee, and C. G. Sodini, “Carotid arterial blood pressure waveform monitoring using a portable ultrasound system,” pp. 5692–5695, 2015.

[17] J. Wang, K. Liu, Q. Sun, X. Ni, F. Ai, S. Wang, Z. Yan, and D. Liu, “Diaphragm-based optical fiber sensor for pulse wave monitoring and cardiovascular diseases diagnosis,” Journal of Biophotonics, vol. 12, no. 10, p. e201900084, 2019. [Online]. Available: https://onlinelibrary.wiley.com/doi/abs/10.1002/jbio.201900084

[18] V. Avbelj, “Morphological changes of pressure pulses in oscillometric non-invasive blood pressure measurements,” in 2014 37th International Convention on Information and Communication Technology, Electronics and Microelectronics (MIPRO), 2014, pp. 245–248.

[19] D. A. Hullender and O. R. Brown, “Blood pressure, atrial fibrillation and arterial stiffness data extracted from oscillometric waveform by kalman filtering,” IEEE Transactions on Biomedical Engineering (TBME), 2020.

[20] G. Montfrans, “Oscillometric blood pressure measurement: Progress and problems,” Blood pressure monitoring, vol. 6, pp. 287–290, 2002.

[21] J. J. Miranda et al., “Performance of oscillometric blood pressure devices in childrenin resource-poor settings,,” Eur J Cardiovasc Prev Rehabil., vol. 15, no. 3, pp. 362–364, 2008.

[22] M. Czarkowski et al., “Limitations of the of the oscillometric method for blood pressure measurements in dialyzed patients,,” Medical science monitor, vol. 17, no. 4, pp. MT35–MT40, 2011.

[23] J. Blacher, R. Asmar, S. Djane, G. M. London, and M. E. Safar, “Aortic pulse wave velocity as a marker of cardiovascular risk in hypertensive patients,,” Hypertension AHA, vol. 33, no. 5, pp. 1111–1117, 1999.

[24] W. Li, L. Guerrini, Z. Wang, L. Ma, J. Hu, and D. Ding, “A survey on multisensor fusion and consensus filtering for sensor networks,” Discrete Dynamics in Nature and Society, vol. 2015, Oct. 2015. [Online]. Available: https://doi.org/10.1155/2015/683701

[25] B. Dabul and W. H. Perkins, “The effects of stuttering on systolic blood pressure,” Journal of Speech and Hearing Research, vol. 16, no. 4, pp. 586–591, 1973. [Online]. Available: https://pubs.asha.org/doi/abs/10.1044/jshr.1604.586

[26] Y. Chou, Y. Gu, J. Liu, X. Huang, and J. Lin, “Modelling arterial blood pressure waveforms for extreme bradycardia and tachycardia by curve fitting with gaussian functions,” International Journal of Modelling, Identification and Control, vol. 32, no. 3-4, pp. 226–231, 2019. [Online]. Available: https://www.inderscienceonline.com/doi/abs/10.1504/IJMIC.2019.103651

[27] T. H.-N. Le, T. M. Le, T. Q. Le, and V. Van Toi, “Feature extraction techniques for automatic detection of some specific cardiovascular diseases using ecg: A review and evaluation study,” pp. 543–549, 2020.

[28] S. T. Vistisen, B. Moody, L. A. Celi, and C. Chen, “Post-extrasystolic characteristics in the arterial blood pressure waveform are associated with right ventricular dysfunction in intensive care patients,” Journal of Clinical Monitoring and Computing, 2019.

[29] M. Fasihi, M. H. Nadimi-Shahraki, and A. jannesari, “Multi-class cardiovascular diseases diagnosis from electrocardiogram signals using 1-d convolution neural network,” pp. 372–378, 2020.

[30] N. Paradkar and S. R. Chowdhury, “Primary study for detection of arterial blood pressure waveform components,” pp. 1959–1962, 2015.

[31] T. Ellis, J. McNames, and M. Aboy, “Pulse morphology visualization and analysis with applications in cardiovascular pressure signals,” IEEE Transactions on Biomedical Engineering, vol. 54, no. 9, pp. 1552–1559, 2007.

[32] A. Mahdi, G. D. Clifford, and S. J. Payne, “A model for generating synthetic arterial blood pressure,” Physiological Measurement, vol. 38, no. 3, pp. 477–488, feb 2017. [Online]. Available: https://doi.org/10.1088/1361-6579/aa51b8

[33] I. Moxham, “Understanding arterial pressure waveforms,” Southern African Journal of Anaesthesia and Analgesia, vol. 9, no. 1, pp. 40–42, 2003. [Online]. Available: https://doi.org/10.1080/22201173.2003.10872991

[34] B. Saugel, J. Heeschen, A. Hapfelmeier, S. Romagnoli, and G. Griewe, “Cardiac output estimation using multi-beat analysis of the radial arterial blood pressure waveform: a method comparison study in patients having off-pump coronary artery bypass surgery using intermittent pulmonary artery thermodilution as the reference method,” Journal of Clinical Monitoring and Computing, vol. 34, pp. 649–654, 2020.

[35] S. A. Esper and M. R. Pinsky, “Arterial waveform analysis,” Best Practice Research Clinical Anaesthesiology, pp. 363–380, 2014.

[36] J. B. Mark, Atlas of Cardiovascular Monitoring. New York, NY: Churchill Livingstone Inc., 1998.

[37] E. J. Benjamin, S. S. Virani, C. W. Callaway, et al., “Heart disease and stroke statistics—2018 update,,” American Heart Association. Circulation., no. 137, p. e67–e492, 2018.

[38] D. E. Newman-Toker, Z. Wang, Y. Zhu, N. Nassery, A. S. S. Tehrani, A. C. Schaffer, C. W. Yu-Moe, G. D. Clemens, M. Fanai, and D. Siegal, “Rate of diagnostic errors and serious misdiagnosis-related harms for major vascular events, infections, and cancers: toward a national incidence estimate using the “big three”,” Diagnosis, vol. 8, no. 1, pp. 67–84, 2021. [Online]. Available: https://doi.org/10.1515/dx-2019-0104

[39] G. R. Quinn, D. Ranum, E. Song, M. Linets, C. Keohane, H. Riah, and P. Greenberg, “Missed diagnosis of cardiovascular disease in outpatient general medicine: Insights from malpractice claims data,” The Joint Commission Journal on Quality and Patient Safety, vol. 43, no. 10, pp. 508–516, 2017. [Online]. Available: https://www.sciencedirect.com/science/article/pii/S1553725017301162

[40] G. E. McVeigh, C. W. Bratteli, D. J. Morgan, C. M. Alinder, S. P. Glasser, S. M. Finkelstein, and J. N. Cohn, “Age-related abnormalities in arterial compliance identified by pressure pulse contour analysis,” Hypertension, vol. 33, no. 6, pp. 1392–1398, 1999.

[41] A. S. Desai and L. W. Stevenson, “Rehospitalization for heart failure,” Circulation, vol. 126, no. 4, pp. 501–506, 2012. [Online]. Available: https://www.ahajournals.org/doi/abs/10.1161/CIRCULATIONAHA.112.125435

[42] M. Moon, “Us tops 16 nations in stemi readmissions,” CardiologyNews. February, vol. 30, 2012.

[43] M. McKinney, “Preparing for impact. many hospitals will struggle to escape or absorb penalty for readmissions.” Modern Healthcare, vol. 42, pp. 6–7, 2012.

[44] R. A. Berenson, R. A. Paulus, and N. S. Kalman, “Medicare’s readmissions-reduction program—a positive alternative,” New England Journal of Medicine, vol. 366, no. 15, pp. 1364–1366, 2012.

[45] Why do we really need pressure suits? [Online]. Available: https://www.nasa.gov/sites/default/files/atoms/files/dressingforaltitude.pdf

[46] Physics of diving. [Online]. Available: https://www.ehs.ucsb.edu/files/docs/ds/physics.pdf

[47] H. Crawford, “Survivable impact forces on human body constrained by full body harness.” [Online]. Available: https://www.hse.gov.uk/research/hslpdf/2003/hsl03– 09.pdf

[48] W. Wyatt Hoback, A. Pursley, K. Farnsworth-Hoback, and L. G. Higley, “A Laboratory Exercise to Explore Sustained Gravitational-Force Tolerance by Insects,” The American Biology Teacher, vol. 77, no. 9, pp. 707–709, 11 2015. [Online]. Available: https://doi.org/10.1525/abt.2015.77.9.11

[49] J. R. K. Zipf and K. L. Cashdollar, “Effects of blast pressure on structures and the human body.”

[50] D. A. Hullender, Dynamic Systems Modeling and Simulation - Theory and Examples., 18th ed. The University of Texas at Arlington, 2019.

[51] J. Juran and A. Godfrey, Juran’s Quality Handbook, ser. McGrawHill Handbooks. McGraw-Hill Education, 1999. [Online]. Available: https://books.google.com/books?id=moURDQAAQBAJ

[52] F. L. Lewis, L. Xie, and D. Popa, Eds., Optimal and Robust Estimation. Boca Raton, FL: CRC Press., 2008.

[53] Mayo Clinic Staff. High blood pressure - hypertension,. [Online]. Available: https://www.mayoclinic.org/diseases-conditions/high-bloodpressure/symptoms-causes/syc-20373410?p=1

[54] T. R. Dawber, H. E. THomas Jr, and P. M. McNamara, “Characteristics of the dicrotic notch of the arterial pulse wave in coronary heart disease,” Angiology, vol. 24, no. 4, pp. 244–255, 1973.

[55] P. Wood, “Aortic stenosis,” The American Journal of Cardiology, vol. 1, no. 5, pp. 553–571, 1958, seventh Annual Meeting. [Online]. Available: https://www.sciencedirect.com/science/article/pii/0002914958901383

[56] D. Garcia, P. Pibarot, L. Kadem, and L.-G. Durand, “Respective impacts of aortic stenosis and systemic hypertension on left ventricular hypertrophy,” Journal of Biomechanics, vol. 40, no. 5, pp. 972–980, 2007. [Online]. Available: https://www.sciencedirect.com/science/article/pii/S0021929006001199

[57] E. J. da S. Luz, W. R. Schwartz, G. Ca´mara-Ch´avez, and D. Menotti, “Ecg-based heartbeat classification for arrhythmia detection: A survey,” Computer Methods and Programs in Biomedicine, vol. 127, pp. 144–164, 2016. [Online]. Available: https://www.sciencedirect.com/science/article/pii/S0169260715003314

[58] N. Thakor and Y.-S. Zhu, “Applications of adaptive filtering to ecg analysis: noise cancellation and arrhythmia detection,” IEEE Transactions on Biomedical Engineering, vol. 38, no. 8, pp. 785–794, 1991.

[59] E. L. Pritchett, “Management of atrial fibrillation,” New England Journal of Medicine, vol. 326, no. 19, pp. 1264–1271, 1992.

[60] S. Nattel, “New ideas about atrial fibrillation 50 years on,” Nature, vol. 415, no. 6868, pp. 219–226, 2002.

[61] G. Van Der Hoeven, P. Clerens, J. Donders, J. Beneken, and J. Vonk, “A study of systolic time intervals during uninterrupted exercise.” Heart, vol. 39, no. 3, pp. 242–254, 1977.

[62] R. P. Lewis, S. Rittogers, W. Froester, and H. Boudoulas, “A critical review of the systolic time intervals.” Circulation, vol. 56, no. 2, pp. 146–158, 1977.

[63] D. H. Spodick, “Normal sinus heart rate: appropriate rate thresholds for sinus tachycardia and bradycardia,” Southern medical journal, vol. 89, no. 7, p. 666—667, July 1996. [Online]. Available: https://doi.org/10.1097/00007611-199607000-00003

[64] M. Brandfonbrener, M. LANDOWNE, and N. W. SHOCK, “Changes in cardiac output with age,” Circulation, vol. 12, no. 4, pp. 557–566, 1955.

[65] J.-L. Vincent, “Understanding cardiac output,” Critical care, vol. 12, no. 4, pp. 1–3, 2008.

[66] J. R. McDonough, R. A. Danielson, R. E. Wills, and D. L. Vine, “Maximal cardiac output during exercise in patients with coronary artery disease,” The American journal of cardiology, vol. 33, no. 1, pp. 23–29, 1974.

[67] A.-M. Salmasi, “Cardiac output in coronary artery disease,” Cardiac output and regional flow in health and disease, pp. 127–135, 1993.

[68] C. W. Hogue Jr, S. F. Murphy, K. B. Schechtman, and V. G. D´avila-Rom´an, “Risk factors for early or delayed stroke after cardiac surgery,” Circulation, vol. 100, no. 6, pp. 642–647, 1999

[69] C. Meune, Y. Allanore, J.-Y. Devaux, O. Dessault, D. Duboc, S. Weber, and A. Kahan, “High prevalence of right ventricular systolic dysfunction in early systemic sclerosis.” The Journal of rheumatology, vol. 31, no. 10, pp. 1941–1945, 2004.

[70] S. Lambova, “Cardiac manifestations in systemic sclerosis,” World journal of cardiology, vol. 6, no. 9, p. 993, 2014.

[71] J. Jansen, K. Wesseling, J. Settels, and J. Schreuder, “Continuous cardiac output monitoring by pulse contour during cardiac surgery,” European heart journal, vol. 11, no. suppl I, pp. 26–32, 1990.

[72] T. Collis, R. B. Devereux, M. J. Roman, G. de Simone, J.-L. Yeh, B. V. Howard, R. R. Fabsitz, and T. K. Welty, “Relations of stroke volume and cardiac output to body composition: the strong heart study,” Circulation, vol. 103, no. 6, pp. 820–825, 2001.

[73] G. L. Evans, H. Smulyan, and R. H. Eich, “Role of peripheral resistance in the control of cardiac output,” The American journal of cardiology, vol. 20, no. 2, pp. 216–221, 1967.

[74] P.-O. ˚Astrand, T. E. Cuddy, B. Saltin, and J. Stenberg, “Cardiac output during submaximal and maximal work,” Journal of Applied Physiology, vol. 19, no. 2, pp. 268–274, 1964.

[75] N. L. Mills, J. J. R. Miller, A. Anand, S. D. Robinson, G. A. Frazer, D. Anderson, L. Breen, I. B. Wilkinson, C. M. McEniery, K. Donaldson, D. E. Newby, and W. MacNee, “Increased arterial stiffness in patients with chronic obstructive pulmonary disease: a mechanism for increased cardiovascular risk,” Thorax, vol. 63, pp. 306 – 311, 2007.

[76] M. Nirmalan and P. M. Dark, “Broader applications of arterial pressure wave form analysis,” Continuing Education in Anaesthesia Critical Care Pain, vol. 14, no. 6, pp. 285–290, 02 2014. [Online]. Available: https://doi.org/10.1093/bjaceaccp/mkt078

[77] T. P. JUDGE and J. W. KENNEDY, “Estimation of aortic regurgitation by diastolic pulse wave analysis,” Circulation, vol. 41, no. 4, pp. 659–665, 1970. [Online]. Available: https://www.ahajournals.org/doi/abs/10.1161/01.CIR.41.4.659

[78] H. N. Sabbah and P. D. Stein, “Valve origin of the aortic incisura,” The American Journal of Cardiology, vol. 41, no. 1, pp. 32–38, 1978. [Online]. Available: https://www.sciencedirect.com/science/article/pii/0002914978901285

[79] A. Yartsev, “Interpretation of abnormal arterial line waveforms.” [Online]. Available: https://derangedphysiology.com/main/cicm-primary-exam/requiredreading/cardiovascular-system/Chapter%20761/interpretation-abnormal-arterialline-waveforms

[80] P. S. Saba, M. J. Roman, A. Ganau, R. Pini, E. C. Jones, T. G. Pickering, and R. B. Devereux, “Relationship of effective arterial elastance to demographic and arterial characteristics in normotensive and hypertensive adults.” Journal of hypertension, vol. 13, no. 9, pp. 971–977, 1995.

[81] E. Hermeling, R. S. Reneman, A. P. Hoeks, and K. D. Reesink, “Advances in arterial stiffness assessment,” Artery Research, vol. 5, no. 4, pp. 130–136, 2011.

[82] F. Hatib, Z. Jian, S. Buddi, C. Lee, J. Settels, K. Sibert, J. Rinehart, and M. Cannesson, “Machine-learning algorithm to predict hypotension based on high-fidelity arterial pressure waveform analysis,” Anesthesiology, vol. 129, no. 4, pp. 663–674, 2018.

[83] M. R. Joffres, P. Hamet, D. R. MacLean, G. J. L’italien, and G. Fodor, “Distribution of blood pressure and hypertension in canada and the united states,” American Journal of Hypertension, vol. 14, no. 11, pp. 1099–1105, 2001.

[84] L. Tin, D. Beevers, and G. Lip, “Systolic vs diastolic blood pressure and the burden of hypertension,” Journal of human hypertension, vol. 16, no. 3, pp. 147–150, 2002.

[85] C. E. BEMIS, R. Gorlin, H. G. KEMP, and M. V. HERMAN, “Progression of coronary artery disease: a clinical arteriographic study,” Circulation, vol. 47, no. 3, pp. 455– 464, 1973.

[86] D.-W. Park, R. M. Clare, P. J. Schulte, K. S. Pieper, L. K. Shaw, R. M. Califf, E. M. Ohman, F. Van de Werf, S. Hirji, R. A. Harrington, et al., "Extent, location, and clinical significance of non–infarct-related coronary artery disease among patients with st-elevation myocardial infarction," Jama, vol. 312, no. 19, pp. 2019–2027, 2014.

[87] C. Berthe, L. A. Pierard, M. Hiernaux, G. Trotteur, P. Lempereur, J. Carlier, and H. E. Kulbertus, "Predicting the extent and location of coronary artery disease in acute myocardial infarction by echocardiography during dobutamine infusion," The American journal of cardiology, vol. 58, no. 13, pp. 1167–1172, 1986.

[88] L. Mechtouff, E. Touz´e, P. Steg, E. Ohman, S. Goto, A. Hirsch, J. R¨other, F. Aichner, C. Weimar, D. Bhatt, et al., "Worse blood pressure control in patients with cerebrovascular or peripheral arterial disease compared with coronary artery disease," Journal of internal medicine, vol. 267, no. 6, pp. 621–633, 2010.

[89] "Understanding blood pressure readings." [Online]. Available: https://www.heart.org/en/health-topics/high-blood-pressure/understandingblood-pressure-readings

[90] A. Bur, H. Herkner, M. Vlcek, C. Woisetschlager, U. Derhaschnig, and M. M. Hirschl, "Classification of blood pressure levels by ambulatory blood pressure in hypertension," Hypertension, vol. 40, no. 6, pp. 817–822, 2002.

[91] J. W. Pennebaker, L. Gonder-Frederick, H. Stewart, L. Elfman, and J. A. Skelton, "Physical symptoms associated with blood pressure," Psychophysiology, vol. 19, no. 2, pp. 201–210, 1982. [Online]. Available: https://onlinelibrary.wiley.com/doi/abs/10.1111/j.1469-8986.1982.tb02547.x

[92] Y. Kawano, "Diurnal blood pressure variation and related behavioral factors," Hypertension research, vol. 34, no. 3, pp. 281–285, 2011.

[93] B. S. Buteler, "The relation of systolic upstroke time and pulse pressure in aortic stenosis," 1962.

[94] T. Maruhashi, M. Kajikawa, S. Kishimoto, H. Hashimoto, Y. Takaeko, T. Yamaji, T. Harada, Y. Hashimoto, Y. Han, Y. Aibara, F. M. Yusoff, T. Hidaka, K. Chayama, A. Nakashima, C. Goto, Y. Kihara, and Y. Higashi, "Upstroke time is a useful vascular marker for detecting patients with coronary artery disease among subjects with normal ankle‐brachial index," Journal of the American Heart Association, vol. 9, no. 23, p. e017139, 2020.

[95] M. Bertic, P. Teefy, R. Bagur, and P. Diamantorous, “Variation in aortic pressure upstroke and amplitude in elderly patients with severe symptomatic aortic stenosis with preserved left ventricular ejection fraction,” Canadian Journal of Cardiology, vol. 31, no. 10, Supplement, p. S227, 2015, canadian Cardiovascular Congress 2015. [Online] Available: https://www.sciencedirect.com/science/article/pii/S0828282X15010259

[96] O. Gödje, K. H¨oke, A. E. Goetz, T. W. Felbinger, D. A. Reuter, B. Reichart, R. Friedl, A. Hannekum, and U. J. Pfeiffer, “Reliability of a new algorithm for continuous cardiac output determination by pulse-contour analysis during hemodynamic instability,” Critical care medicine, vol. 30, no. 1, pp. 52–58, 2002.

[97] L. M. Resnick, D. Militianu, A. J. Cunnings, J. G. Pipe, J. L. Evelhoch, R. L. Soulen, and M. A. Lester, “Pulse waveform analysis of arterial compliance: relation to other techniques, age, and metabolic variables,” American journal of hypertension, vol. 13, no. 12, pp. 1243–1249, 2000.

[98] C. F. Babbs, “Oscillometric measurement of systolic and diastolic blood pressures validated in a physiologic mathematical model.” BioMed Eng OnLine, vol. 11, 2012.

[99] R. L. Woods and K. L. Lawrence, Modeling and simulation of dynamic systems. Prentice Hall, 1997.

[100] D. A. Hullender, Dynamic Systems Modeling and Simulation - Homework and Exam Problems., 17th ed. The University of Texas at Arlington, 2019.

[101] (2021, Oct.) Periodic function. [Online]. Available: https://en.wikipedia.org/wiki/Periodic_function

[102] R. E. Kalman, “A new approach to linear filtering and prediction problems,” Transactions of the ASME–Journal of Basic Engineering, vol. 82, no. Series D, pp. 35–45, 1960.

BIOGRAPHICAL STATEMENT

Atul Shrotriya was born in India, in 1994. He received his Bachelor of Technology degree in Mechanical Engineering from the Manipal Institute of Technology, Manipal, India, in 2016. He completed his Master of Science degree in Mechanical Engineering with a focus on control systems from The University of Texas at Arlington in 2021. He worked as a graduate teaching assistant for 2 years (01/2020 to 12/2021) during his master's degree at the University of Texas at Arlington. During his master's degree, he completed a 10-week full-time internship at Smurfit Kappa North America at their Fort Worth location. He acted as an officer of the Engineering Student Council representing over 7400 engineering students throughout his master's degree and was also a part of multiple other leadership and extracurricular activities and/or organizations. Due to multiple research projects with different faculty members, his research and conference presentations include a variety of topics such as trust consensus in coordinated control, evaluation of neuro-fuzzy networks for speech recognition, extended Kalman filter analysis, fault prediction using Kalman filter banks and analysis of blood pressure waveform for detection and diagnosis of cardiovascular anomalies which is the topic of his master's thesis as well. However, all of his research projects are exclusively linked to control systems. He is a member of Pi Tau Sigma honors society and served on the 2021 Student Service Fee Allocation committee appointed to provide recommendations to the President of the University of Texas at Arlington. He also represented the college of engineering at the Student Government - UTA for 3 consecutive semesters. You can find more details about Atul and connect with him directly through his LinkedIn profile at https://www.linkedin.com/in/atul-shrotriya/